Wireless Information and Power Transfer: Energy Efficiency Optimization in OFDMA Systems

Derrick Wing Kwan Ng, *Member, IEEE,* Ernest S. Lo, *Member, IEEE,*
and Robert Schober, *Fellow, IEEE*

Abstract—This paper considers orthogonal frequency division multiple access (OFDMA) systems with simultaneous wireless information and power transfer. We study the resource allocation algorithm design for maximization of the energy efficiency of data transmission (bits/Joule delivered to the receivers). In particular, we focus on power splitting hybrid receivers which are able to split the received signals into two power streams for concurrent information decoding and energy harvesting. Two scenarios are investigated considering different power splitting abilities of the receivers. In the first scenario, we assume receivers which can split the received power into a continuous set of power streams with arbitrary power splitting ratios. In the second scenario, we examine receivers which can split the received power only into a discrete set of power streams with fixed power splitting ratios. For both scenarios, we formulate the corresponding algorithm design as a non-convex optimization problem which takes into account the circuit power consumption, the minimum data rate requirements of delay constrained services, the minimum required system data rate, and the minimum amount of power that has to be delivered to the receivers. By exploiting fractional programming and dual decomposition, suboptimal iterative resource allocation algorithms are developed to solve the non-convex problems. Simulation results illustrate that the proposed iterative resource allocation algorithms approach the optimal solution within a small number of iterations and unveil the trade-off between energy efficiency, system capacity, and wireless power transfer: (1) wireless power transfer enhances the system energy efficiency by harvesting energy in the radio frequency, especially in the interference limited regime; (2) the presence of multiple receivers is beneficial for the system capacity, but not necessarily for the system energy efficiency.

Index Terms—Energy efficiency, green communications, wireless information and power transfer, non-convex optimization.

I. INTRODUCTION

ORTHOGONAL frequency division multiple access (OFDMA) has been widely adopted as the air interface in high speed wireless multiuser communication networks, due to its immunity to channel delay spread and flexibility

in resource allocation. In an OFDMA system, a wideband frequency selective spectrum is converted into a number of orthogonal narrowband frequency flat subcarrier channels which facilitates the multiplexing of users' data and the exploitation of multiuser diversity. On the other hand, next generation communication systems are expected to support multiple users and to guarantee quality of service (QoS). The increasing demand for high data rate and ubiquitous services has led to a high energy consumption in both transmitter(s) and receiver(s). Unfortunately, portable mobile devices are usually only equipped with limited energy supplies (batteries) which creates bottlenecks in perpetuating the lifetime of networks. Besides, the battery capacity has improved at a very slow pace over the past decades and is unable to satisfy the new energy requirements [3]. Consequently, energy-efficient mobile communication system design has become a prominent approach for addressing this issue in energy limited networks [1]–[7]. Specifically, an enormous number of technologies/methods such as energy harvesting and resource allocation optimization have been proposed in the literature for improving the energy efficiency (bits-per-Joule) of wireless communication systems. Among the proposed technologies, energy harvesting from the environment is particularly appealing as it constitutes a perpetual energy source. More importantly, it provides self-sustainability to systems and is virtually free of cost. In practice, numerous renewable energy sources can be exploited for energy harvesting, including solar, tide, geothermal, and wind. However, these natural energy sources are usually location, weather, or climate dependent and may not always be available in enclosed/indoor environments or suitable for mobile devices. On the other hand, wireless power transfer technology, which enables the receivers to scavenge energy from propagating electromagnetic waves (EM) in radio frequency (RF), has gained recent attention in both industry and academia [8]–[14]. Indeed, RF signals carry both information and energy simultaneously. Thus, the RF energy radiated by the transmitter(s) can be recycled at the receivers for prolonging the lifetime of networks. Yet, the utilization of EM waves as a carrier for simultaneous information and power transfer poses many new research challenges for both resource allocation algorithm and receiver design. In [10] and [11], the fundamental trade-off between wireless information and wireless power transfer was studied for flat fading and frequency selective fading, respectively. Specifically, an ideal receiver was assumed in [10] and [11] such that information decoding and energy harvesting can be performed on the
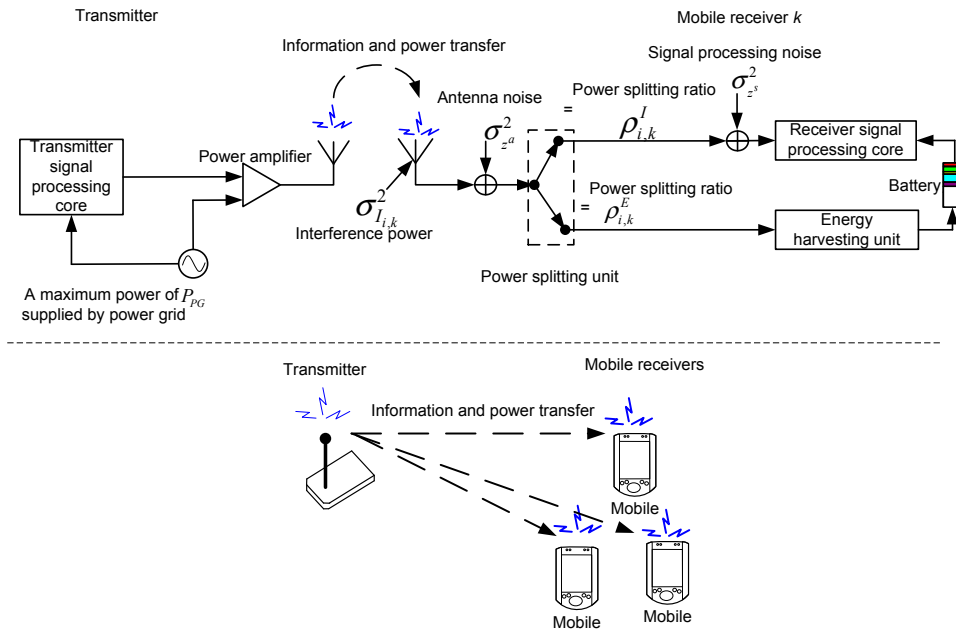
Fig. 1. An OFDMA downlink communication system with $K = 3$ mobile receivers. The upper half of the figure illustrates a block diagram of the transceiver model for wireless information and power transfer.

same received signal which is not possible in practice yet. As a compromise solution, three different types of receivers, namely *power splitting*, *separated*, and *time-switching* receivers, were proposed in [12], [13]. In particular, the *power splitting* receiver splits the received power into two power streams with a certain power splitting ratio for facilitating simultaneous energy harvesting and information decoding in the receiver. The authors in [12] and [13] investigated the rate-energy regions for different types of receivers in two-user and point-to-point single carrier systems, respectively. However, the problem formulations in [12] and [13] do not take into account the heterogeneous data rate requirements of users and the solutions may not meet any data rate requirements and are not applicable to multi-carrier systems with arbitrary numbers of users. On the other hand, the authors in [14] focused on the resource allocation algorithm design for a point-to-point single user system with *power splitting* receiver in ergodic fading channels. Yet, the assumption of channel ergodicity may not be well justified for delay sensitive services in practice since the transmitted data symbols of these services experience slow fading. Besides, the high power consumption in electronic circuitries and RF transmission have been overlooked in [10]–[14] but play an important role in designing energy efficient communication systems [15], [16]. In other words, the energy efficiency of systems with energy harvesting receivers remains unknown. In fact, if a portion of the transmitted RF energy can be harvested by the RF energy harvesting receivers, the system energy efficiency may improve. Yet, the system models adopted in [10]–[14] do not consider the energy recycling process from an energy efficiency point of view. Thus, it is unclear under what conditions energy harvesting receivers improve the system energy efficiency compared to traditional receivers which cannot harvest energy. By incorporating the circuit power consumption and the RF energy harvesting ability of

the receivers into the problem formulation, we presented in [1] and [2] two energy efficient resource allocation algorithms for multicarrier systems employing *separated* receivers and *power splitting* receivers, respectively. Nevertheless, [1] and [2] do not fully exploit the degrees of freedom in resource allocation since data multiplexing of different users on different subcarriers was not considered. Moreover, the algorithm proposed in [2] incurs a high computation complexity at the transmitter since the optimal power splitting ratio is found via full search over a continuous variable. Furthermore, the power splitting ratio may take only discrete levels in practice and the results in [2], which were obtained for continuous power splitting ratios, are not applicable in this case.

In this paper, we address the above issues. To this end, we formulate the resource allocation algorithm design for energy efficient communication in OFDMA systems with simultaneous wireless information and power transfer as an optimization problem. In particular, we focus on the algorithm design for *power splitting* receivers and consider both continuous and discrete power splitting ratios. Besides, data multiplexing of users on different subcarriers is incorporated into the problem formulation. The resulting non-convex optimization problems are solved by iterative algorithms which combine nonlinear fractional programming and dual decomposition. Simulation results illustrate an interesting trade-off between energy efficiency, wireless power transfer, and multiuser diversity.

II. SYSTEM MODEL

In this section, we present the adopted OFDMA signal model and the model for the hybrid information and energy harvesting receiver.

A. OFDMA Channel Model

We consider an OFDMA downlink system in which a transmitter services K mobile receivers. In particular, each

mobile receiver is able to decode information and harvest energy from the received radio signals. All transceivers are equipped with a single antenna, cf. Figure 1. The total system bandwidth is $\mathcal{B}$ Hertz and there are n_F subcarriers. We focus on quasi-static block fading channels and assume that the downlink channel gains can be accurately obtained by feedback from the receivers. The downlink received symbol at receiver $k \in \{1, \ldots, K\}$ on subcarrier $i \in \{1, \ldots, n_F\}$ is given by

$$Y_{i,k} = \sqrt{P_{i,k} l_k g_k} H_{i,k} X_{i,k} + I_{i,k} + Z_{i,k}^a, \quad (1)$$

where $X_{i,k}$, $P_{i,k}$, and $H_{i,k}$ are the transmitted data symbol, the transmitted power, and the multipath fading coefficient from the transmitter to receiver k on subcarrier i, respectively. l_k and g_k represent the path loss and shadowing attenuation from the transmitter to receiver k, respectively. $Z_{i,k}^a$ is the additive white Gaussian noise (AWGN) originating from the antenna on subcarrier i of receiver k. It is modeled as Gaussian random variable with zero mean and variance $\sigma_{z^a}^2$, cf. Figure 1. $I_{i,k}$ is the received aggregate co-channel interference on subcarrier i of receiver k with zero mean and variance $\sigma_{I_{i,k}}^2$. $I_{i,k}$ is emitted by unintended transmitters sharing the same frequency channel.

B. Hybrid Information and Energy Harvesting Receiver

In practice, the model of an energy harvesting receiver depends on its specific implementation. For example, electromagnetic induction and electromagnetic radiation are able to transfer wireless power [11], [14]. Nevertheless, the associated hardware circuitries in the receivers and the corresponding energy harvesting efficiency can be significantly different. Besides, the signal used for decoding the modulated information cannot be used for harvesting energy due to hardware limitations [14]. In order to isolate the resource allocation algorithm design from the specific hardware implementation details, we do not assume a particular type of energy harvesting receiver. In this paper, we focus on receivers which consist of an energy harvesting unit and a conventional signal processing core unit for concurrent energy harvesting and information decoding, cf. Figure 1. In particular, we adopt a receiver which splits the received signal into two power streams [14] in the RF front end with power splitting ratios[1] $\rho_{i,k}^I$ and $\rho_{i,k}^E$. Subsequently, the two power streams with power splitting ratios $\rho_{i,k}^E$ and $\rho_{i,k}^I$ are used for harvesting the energy and decoding the information contained in the signal, respectively. Indeed, by imposing power splitting ratios[2] of $\rho_{i,k}^I = 1, \rho_{i,k}^E = 0$ and $\rho_{i,k}^I = 0, \rho_{i,k}^E = 1$, the hybrid receiver reduces to a tradition information receiver or energy harvesting receiver, respectively. Furthermore, we assume that the harvested energy is used to replenish a rechargeable battery at the receiver. Besides, each receiver has a fixed power consumption of P_{C_R} Watts which is used for maintaining the routine operations in the receiver

and is independent of the amount of harvested power. We note that in practice the receivers may be powered by more than one energy source and the harvested energy may be used as a supplement for supporting the energy consumption[3] of the receivers [17].

III. RESOURCE ALLOCATION - CONTINUOUS SET OF POWER SPLITTING RATIOS

In this section, we consider the resource allocation algorithm design for maximizing the system energy efficiency for the case of a continuous set of power splitting ratios. The derived solution provides not only a useful guideline for choosing a suitable number of discrete power splitting ratios in the power splitting unit, but also serves as a performance benchmark for the case of discrete power splitting ratios. Now, we define the system energy efficiency by first introducing the weighted system capacity and the power dissipation of the system.

A. System Energy Efficiency

Assuming the availability of perfect channel state information (CSI) at the receiver, the channel capacity between the transmitter and receiver k on subcarrier i with subcarrier bandwidth $W = \mathcal{B}/n_F$ is given by[4]

$$\begin{aligned} C_{i,k} &= W \log_2 \left(1 + P_{i,k} \Gamma_{i,k} \right) \quad \text{and} \\ \Gamma_{i,k} &= \frac{\rho_{i,k}^I l_k g_k |H_{i,k}|^2}{\rho_{i,k}^I (\sigma_{z^a}^2 + \sigma_{I_{i,k}}^2) + \sigma_{z^s}^2}, \end{aligned} \quad (2)$$

where $\sigma_{z^s}^2$ is the signal processing noise power at the receiver and $P_{i,k} \Gamma_{i,k}$ is the received signal-to-interference-plus-noise ratio (SINR) on subcarrier i at receiver k.

The *weighted system capacity* is defined as the aggregate number of bits delivered to K receivers and is given by

$$U(\mathcal{P}, \mathcal{S}, \boldsymbol{\rho}) = \sum_{i=1}^{n_F} \sum_{k=1}^{K} \alpha_k s_{i,k} C_{i,k} \quad \text{[bits/s]}, \quad (3)$$

where $\mathcal{P} = \{P_{i,k} \geq 0, \forall i, k\}$ is the power allocation policy, $\mathcal{S} = \{s_{i,k} \in \{0,1\}, \forall i, k\}$ is the subcarrier allocation policy, and $\boldsymbol{\rho} = \{\rho_{i,k}^I, \rho_{i,k}^E \geq 0, \forall i, k\}$ is the power splitting policy with variables $\rho_{i,k}^I$ and $\rho_{i,k}^E$ introduced in Section II-B. $\alpha_k \geq 0, \forall k$, is a non-negative weight which accounts for the priorities of different receivers and is specified by the application layer. In practice, proportional fairness and max-min fairness can be achieved by varying the values of α_k over time[5] [20]. On the other hand, for facilitating the resource allocation algorithm design, we incorporate the total power consumption of the system into the optimization objective function. In particular, the power consumption of the

---

[1]Indeed, $\rho_{i,k}^I$ and $\rho_{i,k}^E$ represent the fractions of the received power of user k on subcarrier i used for information decoding and energy harvesting, respectively. Yet, we follow the convention in the literature [14] and adopt the term "power splitting ratios" in the paper.

[2]In this paper, a perfect passive power splitting unit is assumed; i.e., the power splitting does not incur any power consumption and does not introduce any power loss or signal processing noise to the system.

[3]In this paper, the unit of Joule-per-second is used for energy consumption. Thus, the terms "power" and "energy" are interchangeable.

[4]The received interference signal $I_{i,k}$ on each subcarrier is treated as AWGN in order to simplify the algorithm design [13], [18].

[5]Optimizing the value of α_k for achieving different system objectives is beyond the scope of this paper. Interested readers may refer to [19] for further details.

considered system, $U_{TP}(\mathcal{P}, \mathcal{S}, \boldsymbol{\rho})$, consists of five terms and can be expressed as:

$$U_{TP}(\mathcal{P}, \mathcal{S}, \boldsymbol{\rho}) = P_{C_T} + KP_{C_R} + \sum_{k=1}^{K} \sum_{i=1}^{n_F} \varepsilon P_{i,k} s_{i,k}$$
$$- \sum_{k=1}^{K} Q_{D_k} - \sum_{k=1}^{K} Q_{I_k} \quad \text{[Joule/s]}, \quad (4)$$

where $Q_{D_k} =$

$$\underbrace{\sum_{i=1}^{n_F} \left(\sum_{j=1}^{K} P_{i,j} s_{i,j} \right) l_k g_k |H_{i,k}|^2 \eta_k \rho_{i,k}^E}_{\text{Power harvested from information signal at receiver } k} \quad (5)$$

and $Q_{I_k} = \underbrace{\sum_{i=1}^{n_F} (\sigma_{z^a}^2 + \sigma_{I_{i,k}}^2) \rho_{i,k}^E \eta_k.}_{\substack{\text{Power harvested from interference signal} \\ \text{and antenna noise at receiver } k}} \quad (6)$

The first three terms in (4), i.e., $P_{C_T} + KP_{C_R} + \sum_{k=1}^{K} \sum_{i=1}^{n_F} \varepsilon P_{i,k} s_{i,k}$, represent the power dissipation required for supporting reliable communication. $P_{C_T} > 0$ is the constant *signal processing circuit power consumption* in the transmitters, caused by filters, frequency synthesizer, etc., and is independent of the power radiated by the transmitter. Variables KP_{C_R} and $\sum_{k=1}^{K} \sum_{i=1}^{n_F} \varepsilon P_{i,k} s_{i,k}$ denote the total circuit power consumption in the K receivers and the power dissipation in the power amplifier of the transmitter, respectively. To model the power inefficiency of the power amplifier, we introduce a multiplicative constant, $\varepsilon \geq 1$, for the power radiated by the transmitter in (4) which takes into account the joint effect of the drain efficiency and the power amplifier output backoff [15]. For example, if $\varepsilon = 10$, then 10 Watts of power are consumed in the power amplifier for every 1 Watt of power radiated in the RF; the wasted power during the power amplification is dissipated as heat. On the other hand, the last two terms in (4), i.e., $-\sum_{k=1}^{K} Q_{D_k} - \sum_{k=1}^{K} Q_{I_k}$, represent the harvested energy at the K receivers. The minus sign in front of $\sum_{k=1}^{K} Q_{D_k}$ in (4) indicates that a portion of the power radiated in the RF from the transmitter can be harvested by the K receivers. Besides, $0 \leq \eta_k \leq 1$ in (5) and (6) is a constant which denotes the energy harvesting efficiency of mobile receiver k in converting the received radio signal to electrical energy for storage. In fact, the term $\eta_k l_k g_k |H_{i,k}|^2 \rho_{i,k}^E$ in (5) can be interpreted as a *frequency selective power transfer efficiency* for transferring power from the transmitter to receiver k on subcarrier i. Similarly, the minus sign in front of $\sum_{k=1}^{K} Q_{I_k}$ in (4) accounts for the ability of the receivers to harvest energy from interference signals. The weighted *energy efficiency* of the considered system is defined as the total average number of bits successfully conveyed to the K receivers per Joule consumed energy and is given by

$$U_{eff}(\mathcal{P}, \mathcal{S}, \boldsymbol{\rho}) = \frac{U(\mathcal{P}, \mathcal{S}, \boldsymbol{\rho})}{U_{TP}(\mathcal{P}, \mathcal{S}, \boldsymbol{\rho})} \quad \text{[bits/Joule]}. \quad (7)$$

It is interesting to note that the weighted energy efficiency is a quasi-concave function with respect to the power allocation variables, cf. Appendix A. The quasi-concavity of $U_{eff}(\mathcal{P}, \mathcal{S}, \boldsymbol{\rho})$ can be exploited to show the quasi-concavity of a transformed version of the resource allocation problem, cf. Section III-B, Remark 2. Furthermore, strong interference can act as an energy source which supplies energy to the receivers and facilitates energy savings in the system. This effect is not captured by other system models used in the literature [18], [21]. Therefore, unlike systems with non-energy harvesting receivers, systems with energy harvesting receivers may benefit from interference as far as energy efficiency is concerned. The energy efficiency gain due to the introduction of energy harvesting receivers will be evaluated in the simulation section. On the other hand, we emphasize that the objective function of the considered problem formulation does not capture how the receivers utilize the harvested energy. For instance, if the receivers use the harvested energy for extending their lifetime, an additional system capacity gain may be achieved since the receivers have more time to receive information. In other cases, the receivers may use the harvested energy for uplink transmission which also results in a system capacity gain.

Remark 1: Mathematically, it is possible that $U_{TP}(\mathcal{P}, \mathcal{S}, \boldsymbol{\rho})$ takes a negative value. Yet, $U_{TP}(\mathcal{P}, \mathcal{S}, \boldsymbol{\rho}) > 0$ always holds for the considered system due to the following reasons. First, it can be observed that $\sum_{i=1}^{n_F} \sum_{k=1}^{K} \varepsilon P_{i,k} s_{i,k} \geq \sum_{i=1}^{n_F} \sum_{k=1}^{K} P_{i,k} s_{i,k} > \sum_{k=1}^{K} Q_{D_k}$, where the strict inequality is due to the second law of thermodynamics from physics. In particular, the communication channel between the transmitter and the K receivers is a passive system which does not introduce extra energy. Besides, the energy of the desired signal received at the receiver is attenuated due to path loss and energy scavenging inefficiency. Second, we consider a system where the transmitter and the receivers consume non-negligible amounts of power [16] for signal processing such that $P_{C_T} + KP_{C_R} > \sum_{k=1}^{K} Q_{I_k}$.

B. Optimization Problem Formulation

The optimal power allocation policy, $\mathcal{P}^*$, subcarrier allocation policy, $\mathcal{S}^*$, and power splitting policy $\boldsymbol{\rho}^*$, can be obtained by solving the following optimization problem:

$$\max_{\mathcal{P}, \mathcal{S}, \boldsymbol{\rho}} \quad U_{eff}(\mathcal{P}, \mathcal{S}, \boldsymbol{\rho}) \quad (8)$$

s.t. C1: $Q_{D_k} + Q_{I_k} \geq P_{\min_k}^{\text{req}}, \forall k,$

C2: $\sum_{i=1}^{n_F} \sum_{k=1}^{K} P_{i,k} s_{i,k} \leq P_{\max},$

C3: $P_{C_T} + \sum_{i=1}^{n_F} \sum_{k=1}^{K} \varepsilon P_{i,k} s_{i,k} \leq P_{PG},$

C4: $\sum_{i=1}^{n_F} \sum_{k=1}^{K} s_{i,k} C_{i,k} \geq R_{\min},$

C5: $\sum_{i=1}^{n_F} s_{i,k} C_{i,k} \geq R_{\min_k}, \forall k \in \mathcal{D},$

C6: $P_{i,k} \geq 0, \forall i, k,$ C7: $s_{i,k} \in \{0, 1\}, \forall i, k,$

$$\text{C8: } \sum_{k=1}^{K} s_{i,k} \leq 1, \ \forall i, \quad \text{C9: } \rho_L^E \leq \rho_{i,k}^E \leq \rho_U^E, \forall i, k,$$

$$\text{C10: } \rho_L^I \leq \rho_{i,k}^I s_{i,k} \leq \rho_U^I, \forall i, k,$$

$$\text{C11: } \rho_{i,k}^I s_{i,k} + \rho_{i,k}^E \leq 1, \ \forall i, k, \quad \text{C12: } \rho_{i,k}^E = \rho_{j,k}^E, \ \forall k, i \neq j.$$

Variable $P_{\min_k}^{\mathrm{req}}$ in C1 is a constant which specifies the minimum required power transfer to receiver k. The value of $P_{\max}$ in C2 puts an upper limit on the power radiated by the transmitter. The value of $P_{\max}$ is a constant which depends on the hardware limitations of the power amplifier. C3 limits the maximum power supplied by the power grid for supporting the power consumption of the transmitter to P_{PG}, cf. Figure 1. $R_{\min}$ in C4 is the minimum required data rate of the system. Although $R_{\min}$ is not an optimization variable in this paper, we can strike a balance between the system energy efficiency and the total system throughput by varying its value. In particular, when $R_{\min}$ is increasing, the resource allocator may increase the transmit power for satisfying the higher data rate requirement by sacrificing the system energy efficiency. C5 is the minimum required data rate $R_{\min_k}$ for the *delay constrained* services of receiver k, and is specified by the application layer, and $\mathcal{D}$ denotes a set of receivers having *delay constrained* services. C6 is the non-negative orthant constraint for the power allocation variables. C7 and C8 indicate that each subcarrier can be allocated to at most one receiver exclusively in conveying information; inter-user interference is avoided in the system. Besides, C8 indicates that some subcarriers can be excluded from the subcarrier selection process for energy efficiency maximization. Boundary variables ρ_U^E and ρ_L^E in C9 denote the constant upper and lower bounds of the power splitting ratio for harvesting energy, respectively. The bounds are used to account for the limited capability of the receivers in splitting the received power. Similarly, ρ_U^I and ρ_L^I in C10 denote the constant upper and lower bounds of the power splitting ratio for information decoding where $\rho_U^E + \rho_L^I = 1$ and $\rho_L^E + \rho_U^I = 1$. C11 is the power splitting constraint of the hybrid information and energy harvesting receivers. Its physical meaning is that the power splitting unit, see Figure 1, is a passive device and no extra power gain can be achieved by the power splitting process. C12 constrains the power spitting ratio for energy harvesting, $\rho_{i,k}^E$, such that it is identical for all subcarriers in each receiver. Theoretically, $\rho_{i,k}^E$ can be different across different subcarriers. However, in this case, an analog adaptive passive frequency selective power splitter is required which results in a high system complexity. Therefore, we consider the more practical scenario where $\rho_{i,k}^E = \rho_{j,k}^E, \forall k, \forall j \neq i$. We do not explicitly impose $\rho_{i,k}^I = \rho_{j,k}^I, \forall k, \forall j \neq i$, in the problem formulation. We note that it can be deduced that if both subcarrier i and subcarrier j are allocated to user k for information decoding, $\rho_{i,k}^I = \rho_{j,k}^I$ will hold eventually due to the constraint $\rho_{i,k}^E = \rho_{j,k}^E, \forall k, j \neq i$. However, imposing $\rho_{i,k}^I = \rho_{j,k}^I, \forall k, j \neq i$ explicitly at the very beginning in the problem formulation makes the development for an efficient solution of the optimization problem more cumbersome.

C. Solution of the Optimization Problem

The key challenge in solving (8) is the lack of convexity of the problem formulation. In particular, although the objective function in (8) is quasi-concave with respect to the power allocation variables, the objective function is a jointly non-convex function with respect to $\{\mathcal{P}, \mathcal{S}, \boldsymbol{\rho}\}$. Besides, constraints C1–C12 do not span a convex solution set due to the integer constraint for subcarrier allocation in C7 and the coupled optimization variables in C1. In general, there is no standard approach for solving non-convex optimization problems. In the extreme case, an exhaustive search or branch-and-bound method is needed to obtain the global optimal solution which is computationally infeasible even for small K and n_F. In order to make the problem tractable, we transform the objective function and approximate the transformed objective function in order to simplify the problem. Subsequently, we use the constraint relaxation approach for handling the integer constraint C7 to obtain a close-to-optimal resource allocation algorithm. Next, we introduce the objective function transformation via a parametric approach from nonlinear fractional programming.

D. Transformation of the Objective Function

For notational simplicity, we define $\mathcal{F}$ as the set of feasible solutions[6] of the optimization problem in (8) spanned by constraints C1–C12. Without loss of generality, we assume that $\{\mathcal{P}, \mathcal{S}, \boldsymbol{\rho}\} \in \mathcal{F}$ and we denote q^* as the maximum energy efficiency of the considered system which can be expressed as

$$q^* = \frac{U(\mathcal{P}^*, \mathcal{S}^*, \boldsymbol{\rho}^*)}{U_{TP}(\mathcal{P}^*, \mathcal{S}^*, \boldsymbol{\rho}^*)} = \max_{\mathcal{P}, \mathcal{S}, \boldsymbol{\rho}} \frac{U(\mathcal{P}, \mathcal{S}, \boldsymbol{\rho})}{U_{TP}(\mathcal{P}, \mathcal{S}, \boldsymbol{\rho})}. \quad (9)$$

Now, we introduce the following important Theorem which is borrowed from nonlinear fractional programming [22] for solving the optimization problem in (8).

Theorem 1: The resource allocation policy achieves the maximum energy efficiency q^* if and only if

$$\max_{\mathcal{P}, \mathcal{S}, \boldsymbol{\rho}} \quad U(\mathcal{P}, \mathcal{S}, \boldsymbol{\rho}) - q^* U_{TP}(\mathcal{P}, \mathcal{S}, \boldsymbol{\rho})$$

$$= \quad U(\mathcal{P}^*, \mathcal{S}^*, \boldsymbol{\rho}^*) - q^* U_{TP}(\mathcal{P}^*, \mathcal{S}^*, \boldsymbol{\rho}^*) = 0, \quad (10)$$

for $U(\mathcal{P}, \mathcal{S}, \boldsymbol{\rho}) \geq 0$ and $U_{TP}(\mathcal{P}, \mathcal{S}, \boldsymbol{\rho}) > 0$.

Proof: Please refer to [7, Appendix A] for a proof of Theorem 1.

Theorem 1 provides a necessary and sufficient condition in describing the optimal resource allocation policy. In particular, for an optimization problem with an objective function in fractional form, there exists an equivalent optimization problem with an objective function in subtractive form, e.g. $U(\mathcal{P}, \mathcal{S}, \boldsymbol{\rho}) - q^* U_{TP}(\mathcal{P}, \mathcal{S}, \boldsymbol{\rho})$ in the considered case, such that both problem formulations lead to the same optimal resource allocation policy. Moreover, the optimal resource allocation policy will enforce the equality in (10) which provides an indicator for verifying the optimality of the solution. As a result, we can focus on the equivalent objective function and design a resource allocation policy for satisfying Theorem 1 in the rest of the paper.

---

[6]We assume that the set is non-empty and compact.

TABLE I
ITERATIVE RESOURCE ALLOCATION ALGORITHM.

Algorithm Iterative Resource Allocation Algorithm [Dinkelbach method]

1: Initialization: L_{max} = the maximum number of iterations and Δ = the maximum tolerance
2: Set $q = 0$ and iteration index $j = 0$
3: **repeat** {Iteration Process: Main Loop}
4:   For a given q, obtain an intermediate resource allocation policy $\{\mathcal{P}', \mathcal{S}', \boldsymbol{\rho}'\}$ by solving the problem in (11)
5:   **if** $U(\mathcal{P}', \mathcal{S}', \boldsymbol{\rho}') - qU_{TP}(\mathcal{P}', \mathcal{S}', \boldsymbol{\rho}') < \Delta$ **then**
6:     Convergence = **true**
7:     **return** $\{\mathcal{P}^*, \mathcal{S}^*, \boldsymbol{\rho}^*\} = \{\mathcal{P}', \mathcal{S}', \boldsymbol{\rho}'\}$ and $q^* = \frac{U(\mathcal{P}', \mathcal{S}', \boldsymbol{\rho}')}{U_{TP}(\mathcal{P}', \mathcal{S}', \boldsymbol{\rho}')}$
8:   **else**
9:     Set $q = \frac{U(\mathcal{P}', \mathcal{S}', \boldsymbol{\rho}')}{U_{TP}(\mathcal{P}', \mathcal{S}', \boldsymbol{\rho}')}$ and $j = j + 1$
10:    Convergence = **false**
11: **end if**
12: **until** Convergence = **true** or $j = L_{max}$

E. Iterative Algorithm for Energy Efficiency Maximization

In this section, an iterative algorithm (known as the Dinkelbach method[7] [22]) is proposed for solving (8) with an equivalent objective function such that the obtained solution satisfies the conditions stated in Theorem 1. The proposed algorithm is summarized in Table I (on the next page) and the convergence to the optimal energy efficiency is guaranteed if the inner problem (11) is solved in each iteration.

Proof: Please refer to [7, Appendix B] for a proof of convergence.

As shown in Table I, we solve the following optimization problem for a given parameter q in each iteration in the main loop, i.e., lines 3–12:

$$\max_{\mathcal{P}, \mathcal{S}, \boldsymbol{\rho}} \quad U(\mathcal{P}, \mathcal{S}, \boldsymbol{\rho}) - qU_{TP}(\mathcal{P}, \mathcal{S}, \boldsymbol{\rho})$$
$$\text{s.t. C1 - C12.} \tag{11}$$

We note that for any value of q generated by Algorithm I in each iteration, $U(\mathcal{P}, \mathcal{S}, \boldsymbol{\rho}) - qU_{TP}(\mathcal{P}, \mathcal{S}, \boldsymbol{\rho}) \geq 0$ is always valid; negative energy efficiencies will not occur. Please refer to [7, Proposition 3] for a proof. In fact, the transformed objective function, i.e., $U(\mathcal{P}, \mathcal{S}, \boldsymbol{\rho}) - qU_{TP}(\mathcal{P}, \mathcal{S}, \boldsymbol{\rho})$, has an interesting pricing interpretation from the field of economics. In particular, $U(\mathcal{P}, \mathcal{S}, \boldsymbol{\rho})$ indicates the system profit due to information transmission while $qU_{TP}(\mathcal{P}, \mathcal{S}, \boldsymbol{\rho})$ represents the associated cost due to energy consumption. Besides, the terms Q_{D_k} and Q_{I_k} in $U_{TP}(\mathcal{P}, \mathcal{S}, \boldsymbol{\rho})$ are the corresponding rebate and discount to the energy cost via energy harvesting, respectively. The optimal value of q represents a scaling factor for balancing profit and cost.

1) Solution of the Main Loop Problem (11): The transformed problem has an objective function in subtractive form and is parameterized by variable q. Unfortunately, there are

still two obstacles in tackling the problem. First, the power splitting variables for information decoding and energy harvesting, i.e., $\rho_{i,k}^I$ and $\rho_{i,k}^E$, are coupled with the power allocation variables in both the objective function and constraint C1 which complicates the solution. Second, the combinatorial constraint C7 on the subcarrier allocation variables creates a disjoint feasible solution set which is a hurdle for solving the problem via tools from convex optimization. In order to derive a tractable resource allocation algorithm, we approximate the transformed objective function in the following. First, we approximate the *weighted system capacity* as

$$U(\mathcal{P}, \mathcal{S}, \boldsymbol{\rho}) = \sum_{i=1}^{n_F} \sum_{k=1}^{K} \alpha_k s_{i,k} W \log_2 \left(1 + P_{i,k}\Gamma_{i,k}\right)$$
$$\approx \widehat{U}(\mathcal{P}, \mathcal{S}, \boldsymbol{\rho}) \tag{12}$$

where $\widehat{U}(\mathcal{P}, \mathcal{S}, \boldsymbol{\rho}) = \sum_{i=1}^{n_F} \sum_{k=1}^{K} \alpha_k s_{i,k} W \log_2 \left(P_{i,k}\Gamma_{i,k}\right) \tag{13}$

which is a tight approximation for high SINR[8], i.e., $P_{i,k}\Gamma_{i,k} \gg 1$. On the other hand, we adopt a lower bound on $U_{TP}(\mathcal{P}, \mathcal{S}, \boldsymbol{\rho})$ in the transformed objective function in (11):

$$U_{TP}(\mathcal{P}, \mathcal{S}, \boldsymbol{\rho})$$
$$\geq \widehat{U}_{TP}(\mathcal{P}, \mathcal{S}, \boldsymbol{\rho}) = P_{C_T} + KP_{C_R} + \sum_{i=1}^{n_F} \sum_{k=1}^{K} \varepsilon P_{i,k} s_{i,k}$$
$$- \sum_{k=1}^{K} \sum_{i=1}^{n_F} \left(\sum_{j=1}^{K} P_{i,j} s_{i,j}\right) l_k g_k |H_{i,k}|^2 \eta_k - \sum_{k=1}^{K} Q_{I_k}. \tag{14}$$

where $\widehat{U}_{TP}(\mathcal{P}, \mathcal{S}, \boldsymbol{\rho})$ is obtained by setting $\rho_{i,k}^E = 1$ in $U_{TP}(\mathcal{P}, \mathcal{S}, \boldsymbol{\rho})$. Indeed, $\widehat{U}_{TP}(\mathcal{P}, \mathcal{S}, \boldsymbol{\rho})$ can be interpreted as the use of a theoretical receiver which is able to fully recycle and harvest the energy of the signal used for information decoding[9]. As a result, the transformed objective function can be approximated by

$$U(\mathcal{P}, \mathcal{S}, \boldsymbol{\rho}) - qU_{TP}(\mathcal{P}, \mathcal{S}, \boldsymbol{\rho})$$
$$\lesssim \widehat{U}(\mathcal{P}, \mathcal{S}, \boldsymbol{\rho}) - q\widehat{U}_{TP}(\mathcal{P}, \mathcal{S}, \boldsymbol{\rho}). \tag{15}$$

On the other hand, by exploiting constraint C12, we can rewrite constraint C1 in the following form to remove the associated non-convexity:

$$\text{C1:} \quad \sum_{i=1}^{n_F} \left(\sum_{j=1}^{K} P_{i,j} s_{i,j}\right) l_k g_k |H_{i,k}|^2 \eta_k$$
$$+ \sum_{i=1}^{n_F} \sigma_{I_{i,k}}^2 \eta_k \geq \frac{P_{\min_k}^{\text{req}}}{\rho_{1,k}^E}, \forall k, \tag{16}$$

where the right hand side of the inequality in (16) is due to constraint C12: $\rho_{1,k}^E = \rho_{2,k}^E = \ldots = \rho_{i,k}^E = \ldots = \rho_{n_F,k}^E$.

---

[7]We note that the Dinkelbach method is an application of Newton's method for root finding, please refer to [15], [23] for details.

[8]The high SINR assumption is used to bring the optimization problem into convex form which makes the problem mathematically tractable. Indeed, in the proposed problem formulation, a minimum required system data rate $R_{\min}$ is set to guarantee a desired system data rate. Furthermore, we focus on a indoor line of sight communication environment, see Section V. Thus, it is unlikely that a selected receiver has low SINR.

[9]Note that $\rho_{i,k}^E = 1$ is only applied to the received energy harvested from the information signal, but not to the portion harvested from the interference signals.

Besides, we can further simplify the algorithm design by replacing C12 with the following equivalent constraint:

$$\text{C13}: \rho_{1,k}^E = \rho_{r,k}^E, \ \forall k, r \in \{2, \ldots, n_F\}. \quad (17)$$

Next, we handle the combinatorial constraint in C7 by time-sharing relaxation [24], [25]. In particular, we relax the subcarrier selection variable $s_{i,k}$ to be a real value between zero and one instead of a Boolean, i.e., C7: $0 \leq s_{i,k} \leq 1$. As a result, $s_{i,k}$ can be interpreted as a time-sharing factor in allocating subcarrier i to K receivers for delivering information. In addition, we introduce two new auxiliary variables and define them as $\tilde{P}_{i,k} = P_{i,k} s_{i,k}$ and $\tilde{\rho}_{i,k}^I = \rho_{i,k}^I s_{i,k}$. They represent the actual transmitted power and the power splitting ratio for information decoding on subcarrier i for receiver k under the time-sharing condition, respectively. On the other hand, we replace $C_{i,k}$ in C4 and C5 in (11) by $\tilde{C}_{i,k} = W \log_2 \left(\frac{\tilde{P}_{i,k}}{s_{i,k}} \tilde{\Gamma}_{i,k} \right)$, $\tilde{\Gamma}_{i,k} = \Gamma_{i,k} \big|_{\rho_{i,k}^I = \frac{\tilde{\rho}_{i,k}^I}{s_{i,k}}}$ while $C_{i,k} \geq \tilde{C}_{i,k}$. We note that although $C_{i,k} \geq \tilde{C}_{i,k}$ generally holds, $C_{i,k} \approx \tilde{C}_{i,k}$ is asymptotically tight in the high SINR regime. Since the feasible solution set of the problem with $\tilde{C}_{i,k}$ in C4 and C5 is a subset of the original problem [10], the solution obtained with the Dinkelbach method for the approximated objective function can be used as a suboptimal solution to the original optimization problem in (8). Nevertheless, it will be shown in the simulation section that the proposed resource allocation algorithm achieves a close-to-optimal performance in high SINR. Note that by considering the transformed optimization problem with the approximated objective function and relaxed constraint C7 in each iteration of the Dinkelbach method, the proposed scheme converges to the optimal solution of the problem with the approximated objective function introduced in (14).

Remark 2: There is an alternative approach for solving the optimization problem in (8). Instead of using $U(\mathcal{P}, \mathcal{S}, \boldsymbol{\rho}) - qU_{TP}(\mathcal{P}, \mathcal{S}, \boldsymbol{\rho}) \lesssim \widehat{U}(\mathcal{P}, \mathcal{S}, \boldsymbol{\rho}) - q\widehat{U}_{TP}(\mathcal{P}, \mathcal{S}, \boldsymbol{\rho})$ from (15) in each iteration, we could exploit the fact that

$$\frac{U(\mathcal{P}, \mathcal{S}, \boldsymbol{\rho})}{U_{TP}(\mathcal{P}, \mathcal{S}, \boldsymbol{\rho})} \lesssim \frac{\widehat{U}(\mathcal{P}, \mathcal{S}, \boldsymbol{\rho})}{\widehat{U}_{TP}(\mathcal{P}, \mathcal{S}, \boldsymbol{\rho})}.$$

Then, we can use a similar approach as in Appendix A to prove that $\frac{\widehat{U}(\mathcal{P}, \mathcal{S}, \boldsymbol{\rho})}{\widehat{U}_{TP}(\mathcal{P}, \mathcal{S}, \boldsymbol{\rho})}$ is jointly quasi-concave with respect to $(\mathcal{P}, \mathcal{S}, \boldsymbol{\rho})$ under the time-sharing relaxation. As a result, a unique global optimal solution exist and can be obtained by using the bisection method [26]. We note that both approaches achieve the same optimal value.

The problem with transformed objective function in (15) is jointly concave with respect to (w.r.t.) all optimization variables (cf. Appendix B). Besides, it can be further verified that the primal problem satisfies Slater's constraint qualification. As a result, strong duality holds and solving the dual problem is equivalent for solving the primal problem [26]. Motivated

---

[10]In general, the constraint relaxation used in C7 may result in a superset of the feasible solution set. Yet, it will be shown in the next section that the optimal subcarrier allocation policy with respect to the approximated objective function takes values of either zero or one on each subcarrier. In other words, the subcarrier allocation policy is Boolean even though it is allowed to take any real value between zero and one; i.e., the size of the feasible solution set does not change with the constraint relaxation in C7.

by this fact, we solve the primal problem by solving its dual problem in the following.

F. Dual Problem Formulation

In this subsection, the resource allocation policy is derived via solving the dual problem of (11) with approximated objective function. For this purpose, we first need the Lagrangian function of the primal problem. The Lagrangian of (11) is given by

$$\mathcal{L}(\mathbf{w}, \lambda, \gamma, \beta, \boldsymbol{\delta}, \boldsymbol{\upsilon}, \boldsymbol{\mu}, \boldsymbol{\zeta}, \mathcal{P}, \mathcal{S}, \boldsymbol{\rho}) \quad (18)$$

$$= \sum_{i=1}^{n_F} \sum_{k=1}^{K} (\alpha_k + \gamma + \upsilon_k) s_{i,k} \tilde{C}_{i,k} - \lambda \left(\sum_{i=1}^{n_F} \sum_{k=1}^{K} \tilde{P}_{i,k} - P_{\max} \right)$$

$$- q \left(P_{C_T} + K P_{C_R} + \sum_{k=1}^{K} \sum_{i=1}^{n_F} \varepsilon \tilde{P}_{i,k} \right.$$

$$- \sum_{k=1}^{K} \sum_{i=1}^{n_F} \left(\sum_{j=1}^{K} \tilde{P}_{i,j} \right) l_k g_k |H_{i,k}|^2 \eta_k - \sum_{k=1}^{K} Q_{I_k} \right) - \gamma R_{\min}$$

$$- \beta \left(P_{PG} - P_{C_T} + \sum_{i=1}^{n_F} \sum_{k=1}^{K} \varepsilon \tilde{P}_{i,k} \right)$$

$$- \sum_{i=1}^{n_F} \sum_{k=1}^{K} \delta_{i,k} \left(\tilde{\rho}_{i,k}^I + \rho_{i,k}^E - 1 \right) - \sum_{i=1}^{n_F} \zeta_i \left(\sum_{k=1}^{K} s_{i,k} - 1 \right)$$

$$- \sum_{k=1}^{K} \sum_{i=2}^{n_F} \mu_{i,k} \left(\rho_{1,k}^E - \rho_{i,k}^E \right) - \sum_{k \in \mathcal{D}} \upsilon_k R_{\min_k}$$

$$- \sum_{k=1}^{K} w_k \left(\frac{P_{\min_k}^{\text{req}}}{\rho_{1,k}^E} - \sum_{i=1}^{n_F} \left(\sum_{j=1}^{K} \tilde{P}_{i,j} \right) l_k g_k |H_{i,k}|^2 \eta_k - \sum_{i=1}^{n_F} \sigma_{I_{i,k}}^2 \eta_k \right),$$

where $\tilde{C}_{i,k} = W \log_2 \left(\frac{\tilde{P}_{i,k}}{s_{i,k}} \tilde{\Gamma}_{i,k} \right)$ and $\tilde{\Gamma}_{i,k} = \Gamma_{i,k} \big|_{\rho_{i,k}^I = \frac{\tilde{\rho}_{i,k}^I}{s_{i,k}}}$.

$\mathbf{w}$ has elements $w_k \geq 0$, $k \in \{1, \ldots, K\}$, and is the Lagrange multiplier vector corresponding to the individual minimum required power transfer constraint. $\lambda \geq 0$ accounts for the maximum transmit power allowance $P_{\max}$ in constraint C2. $\beta \geq 0$ is the Lagrange multiplier for C3 accounting for the power usage from the power grid at the transmitter. γ is the Lagrange multiplier associated with the minimum data rate requirement of the system in C4. $\boldsymbol{\upsilon}$ denotes the Lagrange multiplier vector for the minimum individual data rate requirement of receiver k in C5 and has elements $\upsilon_k \geq 0, k \in \{1, \ldots, K\}$. We note that $\upsilon_k = 0, \forall k \notin \mathcal{D}$, for the receivers requiring non-delay constrained services. $\boldsymbol{\zeta}$ is the Lagrange multiplier vector accounting for the subcarrier assignment constraint C8 and has elements $\zeta_i, i \in \{1, \ldots, n_F\}$. $\boldsymbol{\delta}$ is the Lagrange multiplier vector for the power splitting constraint C11 and has elements $\delta_{i,k}, i \in \{1, \ldots, n_F\}, k \in \{1, \ldots, K\}$. $\boldsymbol{\mu}$ is the Lagrange multiplier vector for constraint C12 and has elements $\mu_{i,k}, i \in \{1, \ldots, n_F\}, k \in \{1, \ldots, K\}$. On the other hand, the boundary constraints C6, C7, C9, and C10 on the optimization variables are captured by the Karush-Kuhn-Tucker (KKT) conditions when deriving the resource allocation solution in the next section. Thus, the dual problem for the primal problem (11) is given by

$$\min_{\mathbf{w}, \lambda, \gamma, \beta, \boldsymbol{\delta}, \boldsymbol{\upsilon}, \boldsymbol{\zeta} \geq 0, \boldsymbol{\mu}} \ \max_{\mathcal{P}, \mathcal{S}, \boldsymbol{\rho}} \ \mathcal{L}(\mathbf{w}, \lambda, \gamma, \beta, \boldsymbol{\delta}, \boldsymbol{\upsilon}, \boldsymbol{\mu}, \boldsymbol{\zeta}, \mathcal{P}, \mathcal{S}, \boldsymbol{\rho}). \quad (19)$$

G. Dual Decomposition Solution

In this section, the optimal[11] resource allocation policy is obtained via Lagrange dual decomposition [27]. Specifically, the dual problem in (19) is decomposed into a hierarchy of two levels. Level 1, the inner maximization in (19), consists of n_F subproblems with identical structure that can be solved in parallel. Level 2, the outer minimization in (19), is the master problem. The dual problem can be solved iteratively. Specifically, in each iteration, the transmitter solves the n_F subproblems by applying the KKT conditions for a fixed set of Lagrange multipliers. Then the solutions of the subproblems are used for updating the Lagrange multiplier master problem via the gradient method.

Level 1 (Subproblem Solution): Using standard convex optimization techniques and the KKT conditions, for a given q, in each iteration of the Dinkelbach method, the power allocation policy and the power splitting policy on subcarrier i for receiver k are given by

$$\tilde{P}_{i,k}^* = s_{i,k}P_{i,k}^* = s_{i,k}\left[\frac{W(\alpha_k + \gamma + \upsilon_k)}{\ln(2)\left(\Phi_{i,k}\right)}\right]^+, \forall i, k, \quad (20)$$

$$\Phi_{i,k} = q\varepsilon + \beta\varepsilon + \lambda - \sum_{k=1}^{K}(q + w_k)l_k g_k|H_{i,k}|^2\eta_k, \quad (21)$$

$$\rho_{1,k}^{E*} = \left[\sqrt{\left[\frac{w_k P_{\min_k}^{\text{req}}}{\delta_{1,k} - q(\sigma_{z^a}^2 + \sigma_{I_{1,k}}^2)\eta_k + \sum_{j=2}^{n_F}\mu_{j,k}}\right]^+}\right]_{\rho_L^E}^{\rho_U^E}, (22)$$

$\forall k$, and

$$\rho_{j,k}^{E*} = \left[q(\sigma_{z^a}^2 + \sigma_{I_{j,k}}^2)\eta_k - \delta_{j,k} + \mu_{j,k}\right]_{\rho_L^E}^{\rho_U^E}, \quad (23)$$

$\forall k, j \in \{2, \ldots, n_F\}$,

$$\tilde{\rho}_{i,k}^{I*} = s_{i,k}\rho_{i,k}^{I*} = s_{i,k}\left[\frac{\Psi_{i,k}}{2\sqrt{\ln(2)(\delta_{i,k})(\sigma_{z^a}^2 + \sigma_{I_{i,k}}^2)}}\right.$$
$$\left.- \frac{\sigma_{z^s}^2}{2(\sigma_{z^a}^2 + \sigma_{I_{i,k}}^2)}\right]_{\rho_L^I}^{\rho_U^I}, \forall i, k, \quad (24)$$

$$\Psi_{i,k} = \sqrt{4W(\alpha_k + \gamma + \upsilon_k)(\sigma_{z^a}^2 + \sigma_{I_{i,k}}^2) + (\delta_{i,k})\ln(2)\sigma_{z^s}^2}$$
$$\times \sqrt{\sigma_{z^s}^2} \quad (25)$$

and $\mu_{1,k} = 0$. Here, operators $\left[x\right]^+$ and $\left[x\right]_d^c$ are defined as $\left[x\right]^+ = \max\{0, x\}$ and $\left[x\right]_d^c = c$, if $x > c$, $\left[x\right]_d^c = x$, if $d \le x \le c$, $\left[x\right]_d^c = d$, if $d > x$, respectively. The power allocation solution in (20) is known as multilevel water-filling. In particular, the water-level in allocating power on subcarrier i for receiver k, i.e., $\frac{W(\alpha_k + \gamma + \upsilon_k)}{\ln(2)\Phi_{i,k}}$, is not only directly proportional to the priority of receiver k via variable α_k, but also depends on the channel gains of the other $K - 1$ receivers via the term $\sum_{k=1}^{K}(q + w_k)l_k g_k|H_{i,k}|^2\eta_k$. Besides, Lagrange multipliers γ, υ_k, and w_k force the transmitter to transmit with a sufficiently high power to fulfill the system data rate requirement, $R_{\min}$, the individual data rate requirements of

[11]In this section, an optimality refers to the optimality for the problem formulation using the time-sharing assumption and the approximated objective function.

the receivers having delay constrained services, $R_{\min_k}$, and the minimum power transfer requirement, $P_{\min_k}^{\text{req}}$, for receiver k, respectively. Moreover, as can be observed from (20), the power allocation solution $P_{i,k}^*$ is independent of $s_{i,k}$ which facilitates a simple allocation design.

On the other hand, the power splitting ratio for information decoding, $\rho_{i,k}^{I*}$, is also in the form of water-filling and the water-level depends on the priority of the receiver via α_k in (24). Besides, Lagrange multiplier $\mu_{i,k}$ affects the power splitting ratio solution for energy harvesting in (22) and (23) such that $\rho_{1,k}^E$ will eventually equal $\rho_{j,k}^E, \forall j \in \{2, \ldots, n_F\}$, as enforced by consensus constraint C12. Furthermore, when $\sigma_{z^a}^2 + \sigma_{I_{i,k}}^2 \gg \sigma_{z^s}^2$, the SINR on each subcarrier approaches $\frac{P_{i,k}\rho_{i,k}^{I*}l_k g_k|H_{i,k}|^2}{\rho_{i,k}^{I*}(\sigma_{z^a}^2 + \sigma_{I_{i,k}}^2) + \sigma_{z^s}^2} \to \frac{P_{i,k}l_k g_k|H_{i,k}|^2}{\sigma_{z^a}^2 + \sigma_{I_{i,k}}^2}$ and is independent of $\rho_{i,k}^{I*}$. Besides, $\widehat{U}_{TP}(\mathcal{P}, \mathcal{S}, \boldsymbol{\rho})$ is a monotonically decreasing function of $\rho_{i,k}^{E*}$. Therefore, $\rho_{i,k}^{E*} \to \rho_U^E$ and $\rho_{i,k}^{I*} \to \rho_L^I$ become the optimal power splitting policy for energy efficiency maximization. Thus, if $\sigma_{z^a}^2 + \sigma_{I_{i,k}}^2 \gg \sigma_{z^s}^2$ and the lower bound of the power splitting ratio for information decoding is zero, i.e., $\rho_L^I = 0$, then the solution suggests that in this case an infinitesimally small portion of the received power is used at the receivers for information decoding in order to achieve the optimal performance; provided that the data rate constraints C4 and C5 are satisfied. In other words, most of the received power at the receivers should be used for energy harvesting. The above considerations indicate that in the interference limited regime, a hybrid information and energy harvesting receiver must achieve a higher energy efficiency than the traditional pure information receiver. This will be confirmed by simulation in Section V.

On the other hand, subcarrier i is assigned to receiver k when the following selection criterion is satisfied:

$$s_{i,k}^* = \begin{cases} 1 & \text{if } k = \arg\max_a \quad M_{i,a}, \\ 0 & \text{otherwise} \end{cases} \quad (26)$$

where $\quad M_{i,k}$ $\quad (27)$

$$= W\left(\alpha_k + \gamma + \upsilon_k\right)\left[\log_2\left(P_{i,k}^*l_k g_k|H_{i,k}|^2\right)\right.$$
$$+ \log_2\left(\frac{\rho_{i,k}^{I*}}{(\rho_{i,k}^{I*})(\sigma_{z^a}^2 + \sigma_{I_{i,k}}^2) + \sigma_{z^s}^2}\right)$$
$$\left.- \frac{1}{\ln(2)} - \frac{\sigma_{z^s}^2}{\ln(2)(\rho_{i,k}^{I*}(\sigma_{z^a}^2 + \sigma_{I_{i,k}}^2) + \sigma_{z^s}^2)}\right] - \zeta_i$$

is the marginal benefit provided to the system when subcarrier i is assigned to serve receiver k. In other words, receiver k is selected for information transmission on subcarrier i if it can provide the maximum marginal benefit to the system. Besides, if receiver k has a high priority or a stringent individual data rate requirement, it will have high values of α_k or υ_k and the resource allocator at the transmitter will have a higher preference to serve receiver k with subcarrier i. On the other hand, it can be observed from (26) that although constraint relaxation is used in constraint C7 for facilitating the design of the resource allocation algorithm, the subcarrier allocation policy on each subcarrier for the relaxed problem remains Boolean; time sharing does not occur.

Remark 3: The above observation for the optimal power splitting policy in the interference limited regime is valid for

both the problem with the original objective function and the problem with the approximated objective function. Indeed, if the case of an interference limited regime is considered, the use of the approximated objective function is not necessary. Instead, we can first set $\rho_{i,k}^{E*} \to \rho_U^E$ and $\rho_{i,k}^{I*} \to \rho_L^I$ in the problem formulation. $\rho_{i,k}^{E*}$ and $\rho_{i,k}^{I*}$ become constants and the associated non-convexity vanishes. Then, we optimize $\mathcal{P}$ and $\mathcal{S}$ by following a similar approach as used in (8)-(27).

Level 2 (Master Problem Solution): The Level 2 master problem in (19) can be solved by using the gradient method which leads to the following Lagrange multiplier update equations:

$$\lambda(u+1) = \left[\lambda(u) - \xi_1(u) \times \left(P_{\max} - \sum_{i=1}^{n_F}\sum_{k=1}^{K} \tilde{P}_{i,k}\right)\right]^+, \quad (28)$$

$$\beta(u+1) = \left[\beta(u) - \xi_2(u) \times \left(P_{PG} - P_C\right.\right.$$
$$\left.\left. - \sum_{i=1}^{n_F}\sum_{k=1}^{K} \varepsilon\tilde{P}_{i,k}\right)\right]^+, \quad (29)$$

$$\gamma(u+1) = \left[\gamma(u) - \xi_3(u) \times \left(\sum_{i=1}^{n_F}\sum_{k=1}^{K} s_{i,k}\tilde{C}_{i,k}\right.\right.$$
$$\left.\left. - R_{\min}\right)\right]^+, \quad (30)$$

$$\delta_{i,k}(u+1) = \left[\delta_{i,k}(u) - \xi_4(u)\right.$$
$$\left. \times \left(1 - \tilde{\rho}_{i,k}^I - \rho_{i,k}^E\right)\right]^+, \forall i,k, \quad (31)$$

$$\mu_{r,k}(u+1) = \left[\mu_{r,k}(u) - \xi_5(u) \times \left(\rho_{r,k}^E - \rho_{1,k}^E\right)\right], \quad (32)$$
$$\forall r \in \{2,\ldots,n_F\}, \forall k,$$

$$w_k(u+1) = \left[w_k(u) - \xi_6(u)\right.$$
$$\times \left(\sum_{i=1}^{n_F}\left(\sum_{j=1}^{K} \tilde{P}_{i,j}\right) l_k g_k |H_{i,k}|^2 \eta_k\right.$$
$$\left.\left. + \sum_{i=1}^{n_F} \sigma_{I_{i,k}}^2 \eta_k - \frac{P_{\min_k}^{\mathrm{req}}}{\rho_{1,k}^E}\right)\right]^+, \forall k, \quad (33)$$

$$v_k(u+1) = \left[v_k(u) - \xi_7(u) \times \left(\sum_{i=1}^{n_F} s_{i,k}\tilde{C}_{i,k}\right.\right.$$
$$\left.\left. - R_{\min_k}\right)\right]^+, \forall k \in \mathcal{D}, \quad (34)$$

where index $u \geq 0$ is the iteration index and $\xi_t(m)$, $t \in \{1,\ldots,7\}$, are positive step sizes. Then, the updated[12] Lagrange multipliers in (28)–(34) can be used for updating the resource allocation policy in (20)–(27) by solving the n_F subproblems in (19). As the primal problem with the approximated objective function is jointly concave w.r.t. the optimization variables, it is guaranteed that the primal optimal solution can be obtained by solving the problems in Level 1 and Level 2 iteratively, provided that the chosen step sizes, $\xi_t(m)$, are sufficiently small[13]. We note that other than the

---

[12]It can be observed that updating ζ_i is not necessary since it does not affect the result of the subcarrier allocation solution in (26).

[13]In the literature, different methods such as exact line search and back-tracking line search are commonly used for optimizing the step sizes [26], [28]. In this paper, we adopt a backtracking line search approach in optimizing the step sizes for fast convergence.

adopted gradient method, different iterative algorithms such as the ellipsoid method can also be used for finding the optimal Lagrange multipliers due to the convexity of the dual problem [26].

IV. RESOURCE ALLOCATION DESIGN - DISCRETE SET OF POWER SPLITTING RATIOS

In practice, due to the high complexity associated with a high precision power splitting unit, the RF energy harvesting receivers may only be capable of splitting the received power into two power streams based on a finite discrete set of power splitting ratios. In this section, we design a resource allocation algorithm for such receivers. In particular, we assume that there are N distinct power splitting ratios for energy harvesting and information decoding at each receiver. Thus, the power splitting ratios for energy harvesting and information decoding on subcarrier i for mobile receiver k can be represented by the following constraints:

$$\text{C14: } \rho_{i,k}^E \in \{\rho_k^{E_1}, \rho_k^{E_2}, \ldots, \rho_k^{E_n}, \ldots, \rho_k^{E_N}\},$$
$$\text{C15: } \rho_{i,k}^I \in \{\rho_k^{I_1}, \rho_k^{I_2}, \ldots, \rho_k^{I_n}, \ldots, \rho_k^{I_N}\}. \quad (35)$$

$\rho_k^{E_n}$ and $\rho_k^{I_n}$, $n \in \{1,2,\ldots,N\}$, are the possible power splitting modes for energy harvesting and information decoding adopted in receiver k, respectively. The corresponding resource allocation algorithm design can be formulated as the following optimization problem:

$$\max_{\mathcal{P},\mathcal{S},\boldsymbol{\rho}} U_{eff}(\mathcal{P},\mathcal{S},\boldsymbol{\rho})$$
$$\text{s.t.} \quad \text{C1–C8, C11, C12, C14, C15.} \quad (36)$$

Similar to the case of a continuous set of power splitting ratios, the objective function of the above problem formulation inherits the non-convexity of the fractional form of the objective function. Therefore, by using Theorem 1, we can transform the objective function from the fractional form into a subtractive form and solve the problem via the Dinkelbach method. As shown in Table I, in each iteration of the main loop, i.e., lines 3–12, we solve the following optimization problem for a given parameter q:

$$\max_{\mathcal{P},\mathcal{S},\boldsymbol{\rho}} U(\mathcal{P},\mathcal{S},\boldsymbol{\rho}) - qU_{TP}(\mathcal{P},\mathcal{S},\boldsymbol{\rho})$$
$$\text{s.t.} \quad \text{C1–C8, C11, C12, C14, C15.} \quad (37)$$

The additional difficulty in solving the above optimization problem compared to the problem formulation in (8) is the disjoint/discrete nature of the optimization variables $\rho_{i,k}^E$ and $\rho_{i,k}^I$, cf. C14 and C15 in (35). In general, an exhaustive search is required to obtain the global optimal solution and the search space grows in the order of $N^{2K^{n_F}}$, which may not be computationally feasible for systems of moderate size. In the following, we transform (37) into an optimization problem with tractable solution by exploiting subcarrier time-sharing and the concept of power splitting mode selection. In particular, different values of $\rho_k^{I_n}$ can be treated as different operating modes of receiver k with different equivalent SINRs. Then, we combine the subcarrier selection with the operating mode selection by augmenting the dimensions of the optimization variables. To this end, we define the channel capacity between

the transmitter and receiver k on subcarrier i with channel bandwidth W by using power splitting mode n as

$$C_{i,k}^n = W \log_2 \left(1 + P_{i,k}^n \Gamma_{i,k}^n\right) \quad (38)$$

$$\Gamma_{i,k}^n = \frac{\rho_k^{I_n} l_k g_k |H_{i,k}|^2}{\rho_k^{I_n}(\sigma_{z^a}^2 + \sigma_{I_{i,k}}^2) + \sigma_{z^s}^2},$$

and $P_{i,k}^n \Gamma_{i,k}^n$ is the received SINR on subcarrier i at receiver k using power splitting mode n for information decoding. The *weighted system capacity* is defined as the total average number of bits successfully delivered to the K receivers via the N power splitting modes and is given by

$$U(\mathcal{P}^N, \mathcal{S}^N) = \sum_{i=1}^{n_F} \sum_{k=1}^{K} \sum_{n=1}^{N} \alpha_k s_{i,k}^n C_{i,k}^n, \quad (39)$$

where $\mathcal{P}^N = \{P_{i,k}^n \geq 0, \forall i, k, n\}$ is the power allocation policy and $\mathcal{S}^N = \{s_{i,k}^n \in \{0,1\}, \forall i, k, n\}$ is the subcarrier allocation policy for the case of discrete power splitting ratios. We note that the subcarrier allocation policy in (39) incorporates the power splitting mode selection for information decoding. On the other hand, the power consumption of the system can be written as

$$U_{TP}(\mathcal{P}^N, \mathcal{S}^N, \mathcal{A}^N)$$
$$= P_{C_T} + K P_{C_R} + \sum_{i=1}^{n_F} \sum_{k=1}^{K} \sum_{n=1}^{N} \varepsilon P_{i,k}^n s_{i,k}^n$$
$$- \sum_{k=1}^{K} \sum_{n=1}^{N} Q_{D_k}^n - \sum_{k=1}^{K} \sum_{n=1}^{N} Q_{I_k}^n \quad (40)$$

where $Q_{D_k}^n = \underbrace{\sum_{i=1}^{n_F} \left(\sum_{j=1}^{K} \sum_{m=1}^{N} P_{i,j}^m s_{i,j}^m \right) l_k g_k |H_{i,k}|^2 \eta_k \rho_k^{E_n} a_k^n}_{\substack{\text{Power harvested from information signal} \\ \text{at receiver } k \text{ with power splitting mode } n}} \quad (41)$

and $\quad Q_{I_k}^n = \underbrace{\sum_{i=1}^{n_F} (\sigma_{z^a}^2 + \sigma_{I_{i,k}}^2) \rho_k^{E_n} a_k^n \eta_k}_{\substack{\text{Power harvested from interference and} \\ \text{antenna noise at receiver } k \text{ with power splitting mode } n}} \quad . \quad (42)$

Here, $\mathcal{A}^N = \{a_k^n \in \{0,1\}, \forall k, n\}$ is the power splitting ratio selection policy for energy harvesting. In the above problem formulation, a_k^n is the optimization variable which captures the selection of power splitting mode $\rho_k^{E_n}$ for energy harvesting. Similar to the case of the continuous set of power splitting ratios, we consider an approximation of the objective function for facilitating a tractable resource allocation algorithm design in the following. First, the system capacity between the transmitter and the K mobile receivers can be approximated by

$$U(\mathcal{P}^N, \mathcal{S}^N) \overset{(a)}{\approx} \widehat{U}(\mathcal{P}^N, \mathcal{S}^N)$$
$$= \sum_{i=1}^{n_F} \sum_{k=1}^{K} \sum_{n=1}^{N} \alpha_k s_{i,k}^n \widehat{C}_{i,k}^n,$$

$$\widehat{C}_{i,k}^n = W \log_2 \left(P_{i,k}^n \Gamma_{i,k}^n\right) \quad (43)$$

and $\overset{(a)}{\approx}$ in (43) is due to the high SINR assumption. On the other hand, a lower bound for the total power consumption of the system is given by

$$U_{TP}(\mathcal{P}^N, \mathcal{S}^N, \mathcal{A}^N)$$
$$\geq \widehat{U}_{TP}(\mathcal{P}^N, \mathcal{S}^N, \mathcal{A}^N)$$
$$= P_{C_T} + K P_{C_R} + \sum_{k=1}^{K} \sum_{i=1}^{n_F} \sum_{n=1}^{N} \varepsilon P_{i,k}^n s_{i,k}^n$$
$$- \sum_{i=1}^{n_F} \sum_{k=1}^{K} \left(\sum_{j=1}^{K} \sum_{m=1}^{N} P_{i,j}^m s_{i,j}^m \right) l_k g_k |H_{i,k}|^2 \eta_k$$
$$- \sum_{k=1}^{K} \sum_{n=1}^{N} \sum_{i=1}^{n_F} Q_{I_k}^n, \quad (44)$$

where $\widehat{U}_{TP}(\mathcal{P}^N, \mathcal{S}^N, \mathcal{A}^N)$ is obtained by setting $\rho_k^{E_n} a_k^n = 1$. Then, the objective function for the optimization problem for discrete sets of power splitting factors is given by

$$U(\mathcal{P}^N, \mathcal{S}^N) - q U_{TP}(\mathcal{P}^N, \mathcal{S}^N, \mathcal{A}^N)$$
$$\lesssim \widehat{U}(\mathcal{P}^N, \mathcal{S}^N) - q \widehat{U}_{TP}(\mathcal{P}^N, \mathcal{S}^N, \mathcal{A}^N). \quad (45)$$

A. Optimization Problem Formulation

With a slight abuse of notation, we reformulate the optimization problem for discrete power splitting ratios to be solved in each iteration as follows:

$$\max_{\mathcal{P}^N, \mathcal{S}^N, \mathcal{A}^N} \widehat{U}(\mathcal{P}^N, \mathcal{S}^N) - q \widehat{U}_{TP}(\mathcal{P}^N, \mathcal{S}^N, \mathcal{A}^N)$$

s.t. C1: $\sum_{n=1}^{N} Q_{D_k}^n + Q_{I_k}^n \geq P_{\min_k}^{\text{req}}, \forall k,$

C2: $\sum_{i=1}^{n_F} \sum_{k=1}^{K} \sum_{n=1}^{N} P_{i,k}^n s_{i,k}^n \leq P_{\max},$

C3: $P_C + \sum_{i=1}^{n_F} \sum_{k=1}^{K} \sum_{n=1}^{N} \varepsilon P_{i,k}^n s_{i,k}^n \leq P_{PG},$

C4: $\sum_{i=1}^{n_F} \sum_{k=1}^{K} \sum_{n=1}^{N} s_{i,k}^n \widehat{C}_{i,k}^n \geq R_{\min},$

C5: $\sum_{i=1}^{n_F} \sum_{k=1}^{K} \sum_{n=1}^{N} s_{i,k}^n \widehat{C}_{i,k}^n \geq R_{\min_k}, \forall k \in \mathcal{D},$

C6: $P_{i,k}^n \geq 0, \ \forall i, k, n, \quad$ C7: $s_{i,k}^n \in \{0,1\}, \forall i, k, n,$

C8: $\sum_{k=1}^{K} \sum_{n=1}^{N} s_{i,k}^n \leq 1, \ \forall i,$ C9: $a_k^n \in \{0,1\}, \ \forall k, n,$

C10: $\sum_{n=1}^{N} a_k^n = 1, \forall k,$

C11: $\rho_k^{I_n} s_{i,k}^n + \sum_{m=1}^{N} \rho_k^{E_m} a_k^m \leq 1, \ \forall i, k, n,$

C12: $\sum_{m=1}^{N} \rho_k^{I_m} s_{i,k}^m + \rho_k^{E_n} a_k^n \leq 1, \ \forall i, k, n. \quad (46)$

Constraints C1–C6 have the same physical meanings as in the problem formulation in (8). Constraints C7–C12 are imposed to guarantee that in each receiver only one power splitting

mode can be selected for information decoding and energy harvesting. Besides, C11 and C12 indicate that no extra power gain can be achieved in the power splitting process. On the other hand, the non-convexity of the above problem formulation is caused by the coupled optimization variables in C1 and the combinatorial constraints in C7 and C9. In analogy to the techniques used for solving the optimization problem in (11), we solve problem (46) in the following two steps. In the first step, we relax constraints C7 and C9 such that variables $s_{i,k}^n$ and $a_{i,k}^n$ can assume any value between zero and one, i.e., C7: $0 \leq s_{i,k}^n \leq 1, \forall i, k, n$ and C9: $0 \leq a_{i,k}^n \leq 1, \forall i, k, n$. Then $s_{i,k}^n$ and $a_{i,k}^n$ can be interpreted as the time sharing factors for receiver k in utilizing subcarrier i with power splitting mode n. We also define a new variable $\tilde{P}_{i,k}^n = s_{i,k}^n P_{i,k}^n$ for facilitating the design of the resource allocation algorithm. In fact, $\tilde{P}_{i,k}^n$ represents the actual transmit power of the transmitter for receiver k in subcarrier i if power splitting mode n is used under the time sharing condition. In the second step, we replace constraint C1 in (46) by

C1': $\sum_{i=1}^{n_F} \left(\sum_{j=1}^{K} \sum_{m=1}^{N} \tilde{P}_{i,j}^m \right) l_k g_k |H_{i,k}|^2 \eta_k$

$$+ \sum_{i=1}^{n_F} (\sigma_{z^a}^2 + \sigma_{I_{i,k}}^2) \eta_k \geq \frac{a_k^n P_{\min_k}^{\text{req}}}{\rho_k^{E_n}}, \forall k, n. \quad (47)$$

Although C1' is equivalent to C1 in (46) only if a_k^n takes a binary value, i.e., $a_k^n \in \{0, 1\}$, and $\sum_{k=1}^{K} a_k^n = 1$, it will be shown in the next section that the optimal solution for a_k^n has a binary form under constraint C1', despite the adopted constraint relaxation. Consequently, the optimization problem with the approximated objective function and the constraint relaxation is now jointly concave w.r.t. all optimization variables[14]. Besides, it satisfies Slater's constraint qualification. Therefore, we can apply dual decomposition to solve the primal problem via solving its dual problem. The Lagrangian function of the primal problem in (46) is given by

$$\mathcal{L}(\mathbf{w}, \lambda, \gamma, \beta, \boldsymbol{\delta}, \boldsymbol{\upsilon}, \boldsymbol{\varphi}, \boldsymbol{\kappa}, \boldsymbol{\zeta}, \mathcal{P}^N, \mathcal{S}^N, \mathcal{A}^N) \quad (48)$$

$$= \sum_{i=1}^{n_F} \sum_{k=1}^{K} \sum_{n=1}^{N} (\alpha_k + \gamma + \upsilon_k) s_{i,k}^n \widehat{C}_{i,k}^n$$

$$- q \Big(P_{C_T} + K P_{C_R} + \sum_{k=1}^{K} \sum_{n=1}^{N} \sum_{i=1}^{n_F} \varepsilon \tilde{P}_{i,k}^n$$

$$- \sum_{k=1}^{K} \sum_{i=1}^{n_F} \sum_{n=1}^{N} \Big(\sum_{j=1}^{K} \tilde{P}_{i,j}^n \Big) l_k g_k |H_{i,k}|^2 \eta_k - \sum_{k=1}^{K} \sum_{n=1}^{N} Q_{I_k}^n \Big)$$

$$- \gamma R_{\min} - \sum_{i=1}^{n_F} \zeta_i \Big(\sum_{k=1}^{K} \sum_{n=1}^{N} s_{i,k}^n - 1 \Big)$$

$$- \lambda \Big(\sum_{i=1}^{n_F} \sum_{k=1}^{K} \sum_{n=1}^{N} \tilde{P}_{i,k}^n - P_{\max} \Big)$$

[14]The concavity of the above optimization problem can be proved by following a similar approach as in Appendix B for the case of continuous power splitting ratios.

$$- \sum_{i=1}^{n_F} \sum_{k=1}^{K} \sum_{n=1}^{N} \delta_{i,k}^n \Big(\rho_k^{I_n} s_{i,k}^n + \sum_{m=1}^{N} \rho_k^{E_m} a_k^m - 1 \Big)$$

$$- \sum_{i=1}^{n_F} \sum_{k=1}^{K} \sum_{n=1}^{N} \kappa_{i,k}^n \Big(\sum_{m=1}^{N} \rho_k^{I_m} s_{i,k}^m + \rho_k^{E_n} a_k^n - 1 \Big)$$

$$- \sum_{k=1}^{K} \sum_{n=1}^{N} w_k^n \Big(\frac{a_k^n P_{\min_k}^{\text{req}}}{\rho_k^{E_n}} - \sum_{i=1}^{n_F} \Big(\sum_{j=1}^{K} \sum_{m=1}^{N} \tilde{P}_{i,j}^m \Big) l_k g_k |H_{i,k}|^2 \eta_k$$

$$- \sum_{i=1}^{n_F} (\sigma_{z^a}^2 + \sigma_{I_{i,k}}^2) \eta_k \Big) - \sum_{k \in \mathcal{D}} \upsilon_k R_{\min_k}$$

$$- \sum_{k=1}^{K} \varphi_k \Big(\sum_{n=1}^{N} a_k^n - 1 \Big) - \beta \Big(P_{PG} - P_{C_T} + \sum_{i=1}^{n_F} \sum_{k=1}^{K} \sum_{n=1}^{N} \varepsilon \tilde{P}_{i,k}^n \Big),$$

where λ, β, and γ are the scalar Lagrange multipliers associated to constraints C2, C3, and C4 in (46), respectively. $\mathbf{w}, \boldsymbol{\upsilon}, \boldsymbol{\varphi}, \boldsymbol{\delta}$, and $\boldsymbol{\kappa}$ are the Lagrange multiplier vectors for constraints C1', C5, C8, C10, C11, and C12 which have elements $w_k^n \geq 0, n \in \{1, \ldots, N\}, k \in \{1, \ldots, K\}, \upsilon_k \geq 0, \zeta_i \geq 0, i \in \{1, \ldots, n_F\}, \varphi_i, \delta_{i,k}^n$, and $\kappa_{i,k}^n$ respectively. We note that there is no restriction on the value of φ_i since it is associated with equality constraint C10. Thus, the dual problem is given by

$$\min_{\mathbf{w}, \lambda, \gamma, \beta, \boldsymbol{\delta}, \boldsymbol{\upsilon}, \boldsymbol{\zeta}, \boldsymbol{\kappa} \geq 0, \boldsymbol{\varphi}} \quad (49)$$

$$\max_{\mathcal{P}^N, \mathcal{S}^N, \mathcal{A}^N} \mathcal{L}(\mathbf{w}, \lambda, \gamma, \beta, \boldsymbol{\delta}, \boldsymbol{\upsilon}, \boldsymbol{\varphi}, \boldsymbol{\kappa}, \boldsymbol{\zeta}, \mathcal{P}^N, \mathcal{S}^N, \mathcal{A}^N).$$

B. Dual Decomposition Solution

By using dual decomposition and following a similar approach as in Section III-G, the resource allocation policy can be obtained via an iterative procedure. For a given set of Lagrange multipliers $\{\mathbf{w}, \lambda, \gamma, \beta, \boldsymbol{\delta}, \boldsymbol{\upsilon}, \boldsymbol{\varphi}, \boldsymbol{\kappa}, \boldsymbol{\zeta}\}$, the power allocation policy, power splitting policy, and subcarrier allocation policy for receiver k using power splitting mode n on subcarrier i are given by

$$\tilde{P}_{i,k}^{n*} = s_{i,k}^n P_{i,k}^{n*} = s_{i,k} \left[\frac{W(\alpha_k + \gamma + \upsilon_k)}{\ln(2)\left(\Phi_{i,k} \right)} \right]^+, \forall i, k, \quad (50)$$

$$a_k^{n*} = \begin{cases} 1 & \text{if } n = \arg\max_b \ T_k^b \ , \forall k, \\ 0 & \text{otherwise} \end{cases} \quad (51)$$

$$T_k^b = \rho_k^{E_b} \Big(q\eta_k \sum_{i=1}^{n_F} (\sigma_{z^a}^2 + \sigma_{I_{i,k}}^2) - \sum_{i=1}^{n_F} \sum_{m=1}^{N} \delta_{i,k}^m - \sum_{i=1}^{n_F} \kappa_{i,k}^b \Big)$$

$$- \frac{w_k^b P_{\min_k}^{\text{req}}}{\rho_k^{E_b}} - \varphi_k, \quad (52)$$

$$s_{i,k}^{n*} = \begin{cases} 1 & \text{if } n, k = \arg\max_{c,b} \ M_{i,b}^c \ , \forall i, \\ 0 & \text{otherwise} \end{cases} \quad (53)$$

$$
\begin{aligned}
M_{i,k}^n = {} & W\Big(\alpha_k + \gamma + \upsilon_k\Big)\Big[\log_2\Big(P_{i,k}^{n*}l_kg_k|H_{i,k}|^2\Big) \\
& + \log_2\Big(\frac{\rho_k^{I_n}}{\rho_k^{I_n}(\sigma_{z^a}^2 + \sigma_{I_{i,k}}^2) + \sigma_{z^s}^2}\Big) \\
& - \frac{1}{\ln(2)} - \frac{\sigma_{z^s}^2}{\ln(2)(\rho_{i,k}^{I_n}(\sigma_{z^a}^2 + \sigma_{I_{i,k}}^2) + \sigma_{z^s}^2)}\Big] \\
& - \delta_{i,k}^n\rho_k^{I_n} - \Big(\sum_{m=1}^N \kappa_{i,k}^m\Big)\rho_k^{I_n} - \zeta_i
\end{aligned} \tag{54}
$$

and $\Phi_{i,k}$ is defined in (25). The power allocation solution in (50) has a similar multi-level water filling interpretation as in (20). The difference between (20) and (50) is that the power allocation in (50) is performed w.r.t. each power splitting mode. On the other hand, it can be observed from (51) and (53) that the optimal values of a_k^n and $s_{i,k}^n$ are binary numbers, although time sharing relaxation is used for facilitating the algorithm design.

Now, since the dual function is differentiable, we can update the set of Lagrange multipliers for a given set of $\mathcal{P}^N, \mathcal{S}^N, \mathcal{A}^N$ by using the gradient method. The gradient update equations are given by

$$
\begin{aligned}
\lambda(u+1) = {} & \Big[\lambda(u) - \xi_1(u) \times \Big(P_{\max} \\
& - \sum_{i=1}^{n_F}\sum_{k=1}^K\sum_{n=1}^N \tilde{P}_{i,k}^n\Big)\Big]^+,
\end{aligned} \tag{55}
$$

$$
\begin{aligned}
\beta(u+1) = {} & \Big[\beta(u) - \xi_2(u) \times \Big(P_{PG} - P_C \\
& - \sum_{i=1}^{n_F}\sum_{k=1}^K\sum_{n=1}^N \varepsilon\tilde{P}_{i,k}^n\Big)\Big]^+,
\end{aligned} \tag{56}
$$

$$
\begin{aligned}
\gamma(u+1) = {} & \Big[\gamma(u) - \xi_3(u) \times \Big(R_{\min} \\
& - \sum_{i=1}^{n_F}\sum_{k=1}^K\sum_{n=1}^N s_{i,k}^n\widehat{C}_{i,k}^n\Big)\Big]^+,
\end{aligned} \tag{57}
$$

$$
\begin{aligned}
\delta_{i,k}^n(u+1) = {} & \Big[\delta_{i,k}^n(u) - \xi_4(u) \\
& \times \Big(1 - \rho_k^{I_n}s_{i,k}^n - \sum_{m=1}^N \rho_k^{E_m}a_k^m\Big)\Big]^+, \forall i,k,n,
\end{aligned} \tag{58}
$$

$$
\begin{aligned}
\kappa_{i,k}^n(u+1) = {} & \Big[\kappa_{i,k}^n(u) - \xi_5(u) \\
& \times \Big(1 - \sum_{m=1}^N \rho_k^{I_m}s_k^m - \rho_k^{E_k}a_k^n\Big)\Big]^+, \forall i,k,n,
\end{aligned} \tag{59}
$$

$$
\begin{aligned}
w_k^n(u+1) = {} & \Big[w_k^n(u) - \xi_6(u) \\
& \times \Big(\sum_{i=1}^{n_F}\Big(\sum_{j=1}^K \tilde{P}_{i,j}\Big)l_kg_k|H_{i,k}|^2\eta_k \\
& + \sum_{i=1}^{n_F}(\sigma_{z^a}^2 + \sigma_{I_{i,k}}^2)\eta_k - \frac{a_n^kP_{\min_k}^{\text{req}}}{\rho_k^{E_n}},\Big)\Big]^+, \forall k,n,
\end{aligned} \tag{60}
$$

$$
\begin{aligned}
\upsilon_k(u+1) = {} & \Big[\upsilon_k(u) - \xi_7(u) \times \Big(R_{\min_k} \\
& - \sum_{i=1}^{n_F}\sum_{n=1}^N s_{i,k}^n\widehat{C}_{i,k}^n\Big)\Big]^+, \forall k \in \mathcal{D}.
\end{aligned} \tag{61}
$$

Similar to the case of continuous power splitting ratios, updating ζ_i and φ_i is not necessary since they will not affect the power splitting mode selection and subcarrier allocation in (51) and (53), respectively.

V. RESULTS

In this section, simulation results are presented to demonstrate the energy efficiency and system capacity of the proposed resource allocation algorithms. We consider an indoor communication system with K receivers and the corresponding simulation parameters are provided in Table II. We note that the 470 MHz frequency band will be used by IEEE 802.11 for the next generation of Wi-Fi systems [31]. Besides, the wavelength of the carrier signal is 0.6 meter which is smaller than the minimum distance between the transmitter and receivers. Thus, the far-field assumption of the channel model in [29] holds. Furthermore, in practice, the value of circuit power consumption depends on the specific hardware implementation and the application. On the other hand, we assume that all receivers have the same priority $\alpha_k = 1, \forall k$, for illustrating the maximum achievable energy efficiency of the system. The shadowing of all communication links is set to $g_k = 1, \forall k$, to account for the line-of-sight communication setting. Unless specified otherwise, we assume that there is only one receiver requiring delay constrained service with a minimum data rate requirement of $R_{\min_k} = 10$ Mbit/s. In the sequel, the total number of iterations is defined as the number of main loop iterations in the Dinkelbach method. For the case of continuous power splitting ratios, we set $\rho_U^E = \rho_U^I = 1$ and $\rho_L^E = \rho_L^I = 0$. Besides, there are five power splitting ratios for the resource allocation with the discrete set of power splitting ratios: $\rho_{i,k}^E \in \{1, 0.75, 0.5, 0.25, 0\}$ and $\rho_{i,k}^I \in \{0, 0.25, 0.5, 0.75, 1\}$. Moreover, to ensure fast convergence, the step sizes adopted in (28)–(34) and (55)–(61) are optimized via backtracking line search, cf. [26, page 464] and [32, page 230]. Note that if the transmitter is unable to meet the minimum required system data rate $R_{\min}$, the minimum required individual data rate $R_{\min_k}$, or the minimum required power transfer $P_{\min_k}^{\text{req}}$, we set the energy efficiency and the system capacity for that channel realization to zero to account for the corresponding failure. For the sake of illustration, the performance curves of the proposed algorithms for the continuous and discrete sets of power splitting ratios are labeled as "Proposed algorithm I" and "Proposed algorithm II" in Figures 2–7. The average energy efficiency of the system is computed according to (7) and averaged over 100000 independent realizations of multipath fading and path loss attenuation.

A. Convergence and Optimality of Iterative Algorithm

Figure 2 depicts the average system energy efficiency of the proposed iterative algorithms for different levels of received interference versus the number of iterations. Specifically, we are interested in the energy efficiency and convergence speed of the proposed algorithms. We plot the upper bound

TABLE II
SYSTEM PARAMETERS

|	
Maximum service distance $d_{\max}$	10 m
Reference distance d_0	1 m
Users distribution	Uniformly distributed between d_0 and $d_{\max}$
Multipath fading distribution	Rician fading with Rician factor 6 dB
Channel path loss model	TGn path loss model [29]
Carrier center frequency	470 MHz
Number of subcarriers n_F	128
Total bandwidth $\mathcal{B}$ and subcarrier bandwidth W	20 MHz and 156 kHz
Thermal noise power and antenna noise power per subcarrier	-112 dBm and -115 dBm
Quantization noise (12-bit uniform quantizer) per subcarrier	-47 dBm
Minimum system data rate requirement $R_{\min}$	50 Mbit/s
Minimum data rate requirement for delay constrained service $R_{\min_k}$	10 Mbit/s
Class A/B power amplifier [30] with a power efficiency of 16%	$\varepsilon = 6.25$
Maximum power supply P_{PG}	50 dBm
Minimum required power transfer $P_{\min_k}^{\text{req}}$	0 dBm
Energy harvesting efficiency η_k	0.8
Circuit power consumptions: P_{C_T} and P_{C_R}	30 dBm and 20 dBm
Effective antenna gain	12 dB
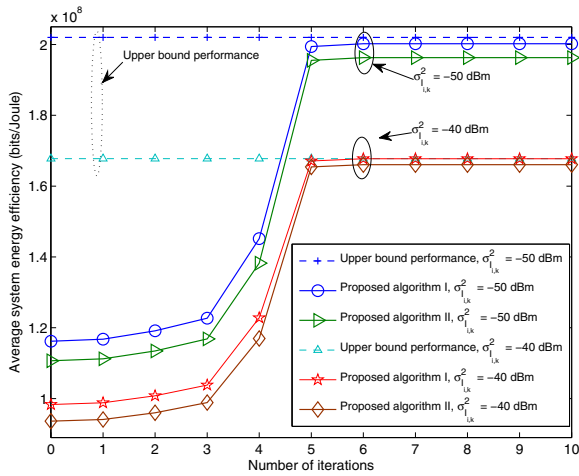
Fig. 2. Average system energy efficiency (bits-per-Joule) versus number of iterations with different levels of interference power, $\sigma_{I_{i,k}}^2$, and $P_{\max} = 30$ dBm. There are $K = 3$ receivers in the system. The dashed solid lines represent the upper bound of energy efficiency after algorithm convergence.

performance[15] of the system after convergence to illustrate the sub-optimality of the proposed algorithms. The dashed lines refer to the average energy efficiency upper bound for each case study. After only 5 iterations, the iterative algorithms achieve over 95% of the upper bound value for all considered scenarios. Besides, the convergence speed of the proposed algorithms is invariant to the interference levels, $\sigma_{I_{i,k}}^2$, which is desirable for practical implementation.

In the following case studies, the number of iterations is set to 5 for illustrating the performance of the proposed algorithms.

B. Energy Efficiency versus Maximum Allowed Transmit Power

Figure 3 shows the average system energy efficiency versus the maximum transmit power allowance, $P_{\max}$, for different received levels of interference, $\sigma_{I_{i,k}}^2$. We first focus on the case of a small number of receivers and moderate interference level. It can be observed that the average system energy efficiency of the proposed algorithms is a monotonically non-decreasing function of $P_{\max}$. In particular, starting from a small value of $P_{\max}$, the energy efficiency first quickly increases with an increasing $P_{\max}$ and then saturates when $P_{\max} > 18$ dBm. This is due to the fact that the two proposed algorithms strike a balance between the system energy efficiency and the power consumption of the system. In fact, once the maximum energy efficiency[16] of the system is achieved, a further increase in the transmit power would result in a degradation in energy efficiency. As expected, proposed algorithm I outperforms proposed algorithm II in all cases since the latter algorithm is designed based on discrete sets of power splitting ratios which span a smaller feasible solution set compared to algorithm I. Besides, Figure 3 reveals that although interference signals can act as a viable energy source to the system, cf. (5) and (7), strong interference impairs the energy efficiency of the system; the energy harvesting gain due to strong interference[17] is unable to compensate the corresponding capacity loss. For comparison, Figure 3 also contains the energy efficiency of two baseline resource allocation schemes. For baseline I, we maximize the weighted system capacity (bit/s) with respect to $\{\mathcal{P}, \mathcal{S}, \boldsymbol{\rho}\}$ subject to constraints C1–C12 in (8), instead of the energy efficiency. Specifically, baseline I focuses on a system with hybrid energy harvesting receivers which split the received signal into two power streams for a finite discrete set of power splitting ratios. On the other hand, baseline II maximizes the weighted energy efficiency of the system with respect to $\{\mathcal{P}, \mathcal{S}\}$ for receivers which do not have energy

---

[15]The upper bound system performance is obtained by directly evaluating the upper bound objective function via replacing the energy consumption function $U_{TP}(\mathcal{P}, \mathcal{S}, \boldsymbol{\rho})$ in (14) by $\widehat{U}(\mathcal{P}, \mathcal{S}, \boldsymbol{\rho})$ for the continuous set of power splitting ratios. We note that the approximation in (12) is asymptotically tight for high SINR.

[16]The maximum energy efficiency refers to the "maximum" w.r.t. the corresponding problem formulation.

[17]Nevertheless, we would like to emphasize that the use of hybrid information and energy harvesting receivers provides a better energy efficiency to the system compared to pure information receivers, as can be observed from baseline II.
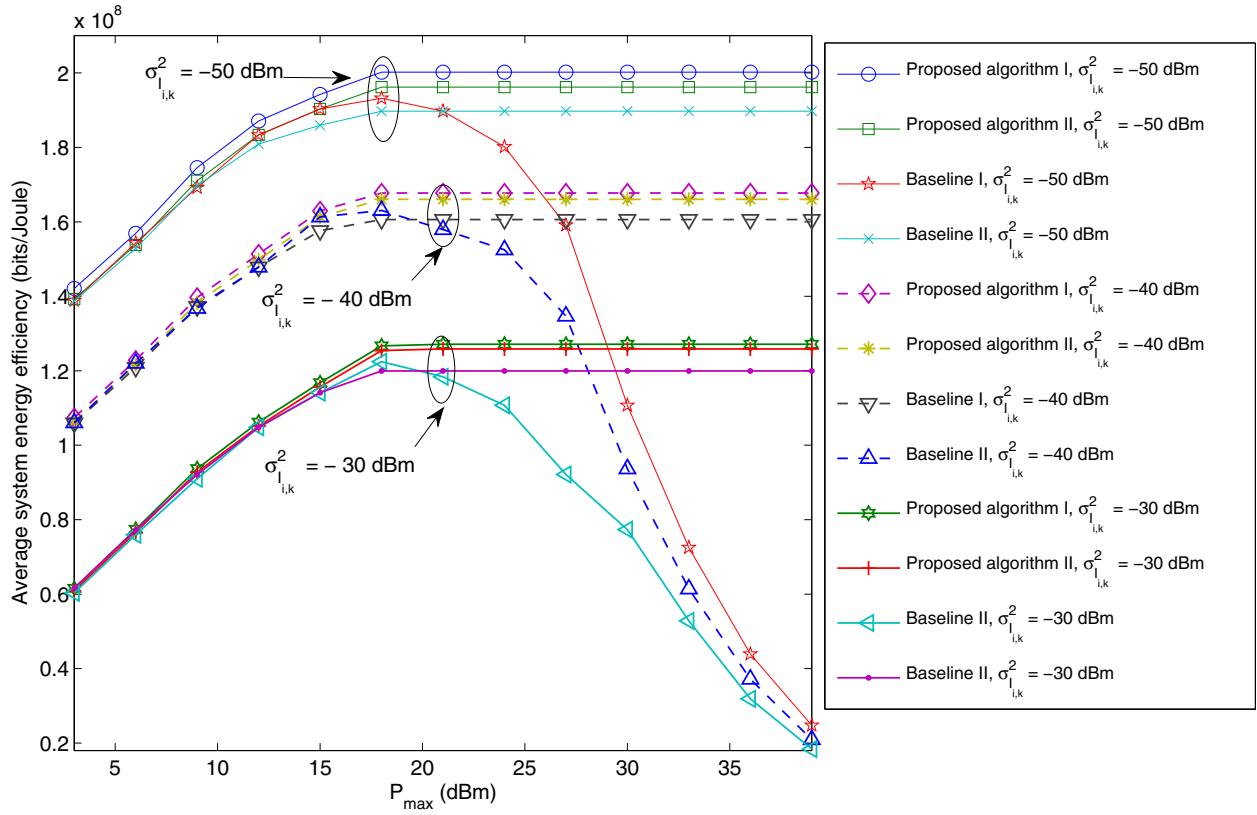
Fig. 3.   Average system energy efficiency (bits-per-Joule) versus maximum transmit power allowance, $P_{\max}$, for $K = 3$ receivers and different levels of interference power, $\sigma_{I_{i,k}}^2$.

harvesting capability. Since the receivers of baseline II are unable to harvest energy, we do not impose constraint C1 for baseline II since a minimum power transfer to the receivers is not required. Figure 3 reveals that in the low transmit power regime and for a small number of receivers, the system with power splitting receivers achieves a small performance gain compared to the system without energy harvesting receivers. This is because in the low transmit power regime, the received power of the desired signal at the receivers may not be sufficiently large for simultaneous information decoding and energy harvesting. As a result, power splitting occurs for fulfilling constraint C1. On the other hand, the energy efficiency gain achieved by the proposed algorithm attains its maximum in the high transmit power allowance regime. It can be observed that approximately a 5% gain in energy efficiency can be achieved for $K = 3$ receivers and a moderate interference power level. We emphasize that in the high transmit power allowance regime, the maximum energy efficiency achieved by the system with hybrid energy harvesting receivers cannot be attained by the system without hybrid energy harvesting receivers (baseline II) via increasing the transmit power.

Now, we focus on the system with a moderate number of receivers and moderate interference levels in the high transmit power allowance regime. Figure 4 illustrates the average system energy efficiency versus the number of receivers for different interference power levels, $\sigma_{I_{i,k}}^2$, and different resource allocation algorithms. The maximum transmit power allowance is set to $P_{\max} = 25$ dBm. In particular, we compare the proposed algorithm II, i.e., energy efficiency maximization

with discrete power splitting ratio receivers, with baseline II. It can be observed from Figure 4 that the performance gain provided by energy harvesting depends on the number of receivers and the interference power level for a fixed maximum transmit power allowance $P_{\max}$. Indeed, when there is only one receiver, the performance gain due to energy harvesting is small since only a small portion of radiated power can be harvested by the receiver. However, when there are more receivers in the systems, more receivers participate in the energy harvesting process and thus a larger amount of energy can be harvested from the RF signals. As a result, a larger performance gain in terms of energy efficiency can be achieved by the proposed algorithm over baseline II when there are more receivers in the system. Furthermore, it can be seen that the performance gain achieved by the proposed algorithm over baseline II increases with the interference power level. The reason behind this is twofold. First, the increase in interference power level provides some extra energy to the system for potential energy harvesting. Second, the strong interference tends to saturate the SINR on each subcarrier such that it is independent of $\rho_{i,k}^{I*}$, i.e., $\frac{P_{i,k}\rho_{i,k}^{I*}l_k g_k |H_{i,k}|^2}{\rho_{i,k}^{I*}(\sigma_{z^a}^2+\sigma_{I_{i,k}}^2)+\sigma_{z^s}^2} \Rightarrow \frac{P_{i,k}l_k g_k |H_{i,k}|^2}{\sigma_{z^a}^2+\sigma_{I_{i,k}}^2}$ for $\sigma_{z^a}^2+\sigma_{I_{i,k}}^2 \gg \sigma_{z^s}^2$. Thus, using more of the received power for information decoding does not provide a significant gain in channel capacity. Consequently, more received power is used for energy harvesting to reduce the total energy consumption of the system (see also Figure 6), which enhances the system energy efficiency. On the other hand, we would like to emphasize that although the energy efficiency gain of algorithm II compared to baseline II depends on the system settings, energy harvesting may be necessary in some applications where other
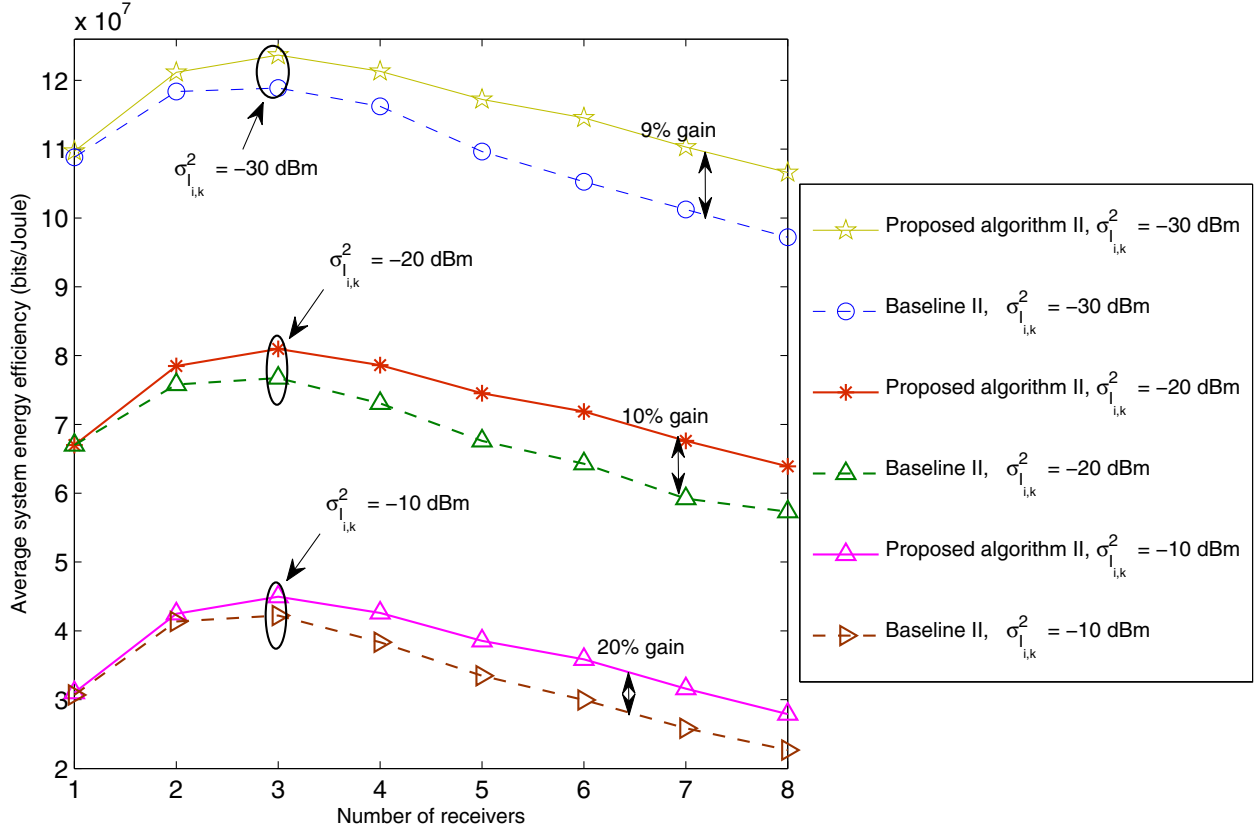
Fig. 4. Average system energy efficiency (bits-per-Joule) versus number of receivers, K, for $P_{\max} = 25$ dBm and different levels of interference power, $\sigma_{I_{i,k}}^2$.

C. Average System Capacity versus Maximum Allowed Transmit Power

In Figure 5, we plot the average system capacity versus the maximum transmit power allowance, $P_{\max}$, for different levels of interference power, $\sigma_{I_{i,k}}^2$. We compare the two proposed algorithms with the two aforementioned baseline schemes. For $P_{\max} < 18$ dBm, it can be observed that the average system capacities of the two proposed algorithms scale with the maximum transmit power allowance $P_{\max}$. Yet, the system capacity gain due to a larger $P_{\max}$ begins to saturate in the high transmit power allowance regime, i.e., $P_{\max} \geq 18$ dBm. Indeed, the proposed algorithms do not further increase the transmit power in the RF if the system capacity gain due to a higher transmit power cannot neutralize the associated energy consumption increase required for boosting the transmit power. Baseline II has a similar behaviour as the proposed algorithms with respect to the maximum transmit power allowance, since baseline II also focuses on energy efficiency maximization. On the other hand, as expected, baseline II achieves a system capacity gain over the other algorithms in the low transmit power allowance regime. Indeed, the SINR of each subcarrier is monotonically increasing with respect to $\rho_{i,k}^I$. In other words, the SINR (capacity) on each subcarrier is maximized when there is no power splitting, i.e., $\rho_{i,k}^I = 1, \rho_{i,k}^E = 0$, which

is the setting for baseline II. We note that although baseline I focuses on system capacity maximization, power splitting occurs for fulfilling constraint C1 which results in a lower system capacity compared to baseline II in the low transmit power regime. However, the system capacity of baseline I is higher than that of the other algorithms in the high transmit power regime, e.g., $P_{\max} \geq 18$ dBm. This is attributed to the fact that in order to maximize the system capacity for baseline I, the transmitters always radiate all the available power. Yet, the higher system capacity of baseline I comes at the expense of a low system energy efficiency, cf. Figure 3. In addition, we observe from Figure 5 that all the considered algorithms are able to fulfill the system data rate requirement in C4 on average.

D. Average Harvested Power versus Maximum Allowed Transmit Power

Figure 6 depicts the average harvested power of the proposed algorithm II versus the maximum allowed transmit power, $P_{\max}$, for different levels of interference power, $\sigma_{I_{i,k}}^2$. It can be seen that in the high transmit power regime, the amount of average harvested power in all considered scenarios is saturated. This is because for the proposed algorithm II, the transmitter stops to increase the transmit power for energy efficiency maximization. Meanwhile, the average interference power level remains unchanged and no extra energy can be harvested by the K receivers. On the other hand, a higher amount of power is harvested by the receivers in the system
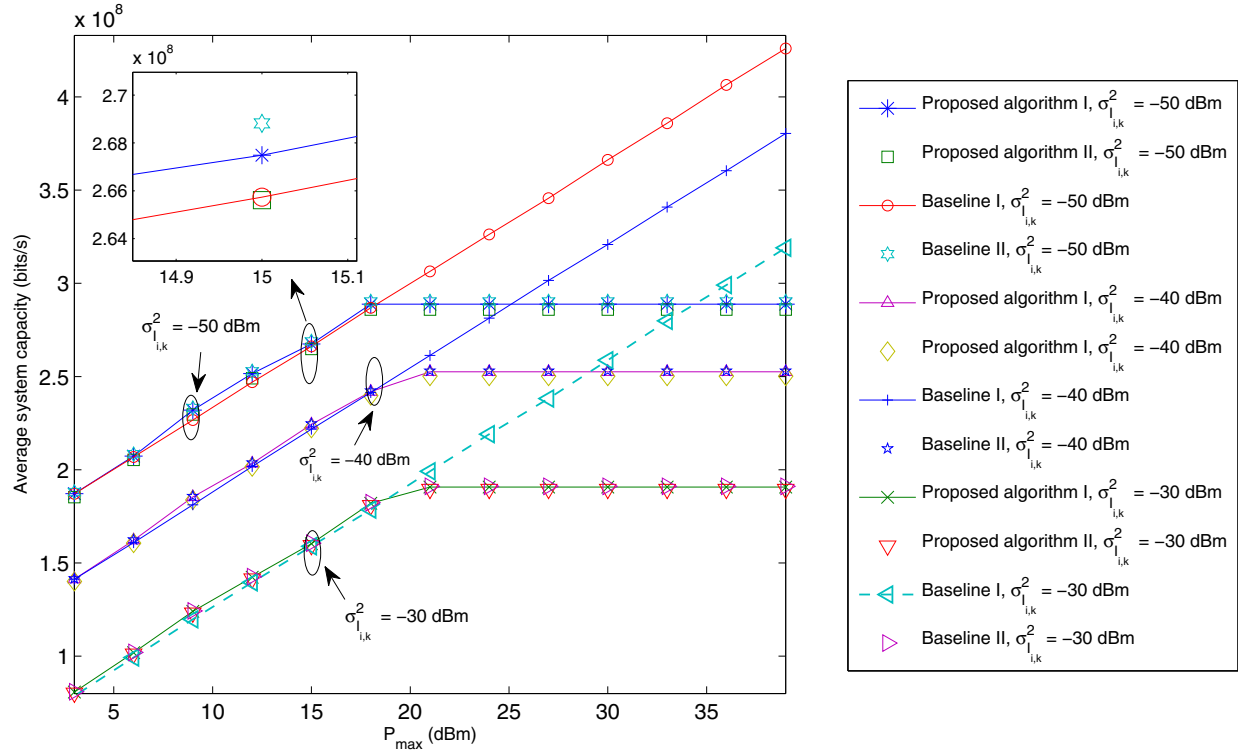
Fig. 5. Average system capacity (bits-per-second) versus maximum transmit power allowance, $P_{\max}$, for different power levels of interference, $\sigma_{I_{i,k}}^2$, and $K = 3$ receivers.

when the interference power level increases as the SINR is independent of $\rho_{I_{i,k}}^k$ on each subcarrier. Thus, splitting more received power for energy harvesting improves system energy efficiency and increases the average harvested power.

E. Average Energy Efficiency and System Capacity versus Number of Receivers

Figure 7(a) and Figure 7(b) illustrate the average system capacity and the average system energy efficiency of the proposed algorithm II versus the number of mobile receivers for different interference power levels, $\sigma_{I_{i,k}}^2$, and different receiver circuit power consumptions, P_{C_R}. In Figure 7(b), it can be observed that the average system capacity increases with the number of receivers in the system since the proposed algorithm is able to exploit multiuser diversity. Specifically, the transmitter has a higher chance of selecting a receiver with good channel conditions when more receivers are in the system, which results in a system capacity gain. In addition, although a higher interference power level impairs the average system capacity, it does not decrease the performance gain due to multiuser diversity as can be concluded from the slopes of the curves. Besides, a higher circuit power consumption in the receivers does not have a large impact on the average system capacity.

On the contrary, Figure 7(a) shows that the average system energy efficiency does not necessarily monotonically increase/decrease w.r.t. the number of receivers. In fact, for a moderate value of receiver circuit power consumption, e.g. $P_{C_R} \geq 15$ dBm, for the considered system setting, the energy
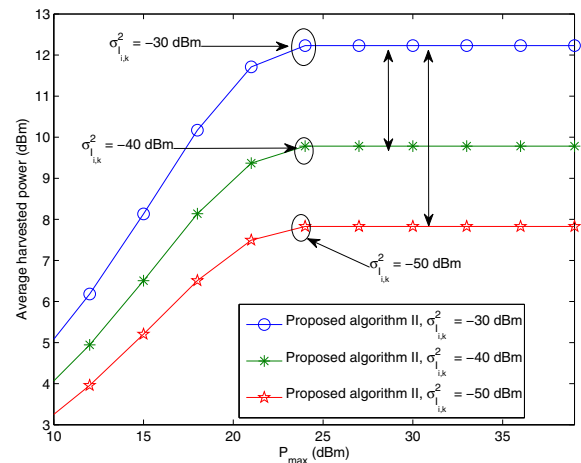

Fig. 6. Average harvested power (dBm) of proposed algorithm II versus the maximum transmit power allowance, $P_{\max}$, for different interference power levels and $K = 3$ receivers. The double-sided arrow indicates the power harvesting gain due to an increasing interference power level.

efficiency of the system first increases and then decreases with an increasing number of receivers. The enhancement of energy efficiency is mainly due to the multiuser diversity gain in the channel capacity when having multiple receivers. Besides, if more receivers participate in the energy harvesting process, a larger portion of energy can be harvested from the RF signals. Nevertheless, an extra circuit energy consumption is incurred by each additional receiver. Indeed, when the
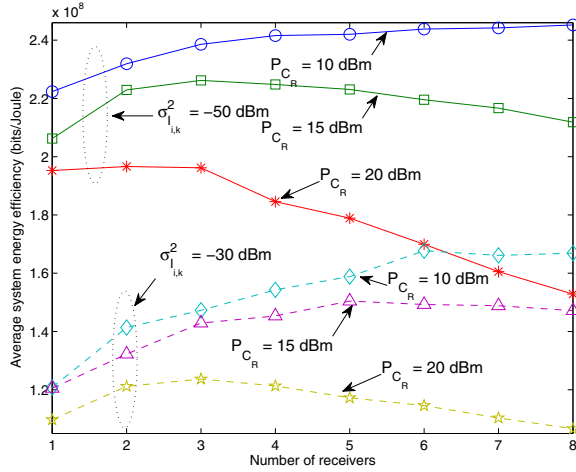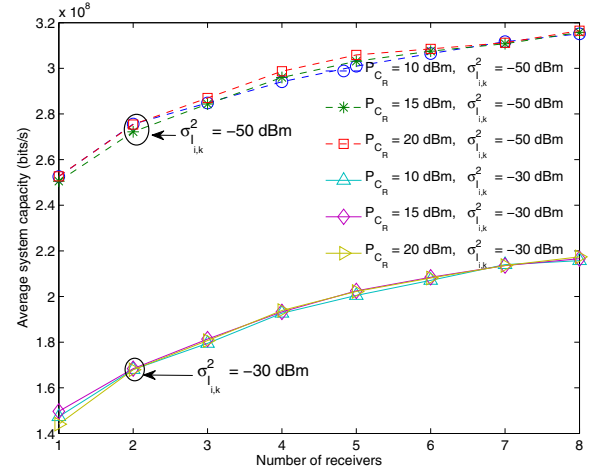
(a) Average energy efficiency (bits-per-Joule) versus K.

(b) Average system capacity (bit-per-second) versus K.

Fig. 7. Average energy efficiency (bits-per-Joule) and average system capacity (bit-per-second) versus the number of receivers K for $P_{\max} = 18$ dBm, different receiver circuit power consumptions, P_{C_R}, and different interference power levels $\sigma^2_{I_{i,k}}$.

number of receivers in the system or P_{C_R} are large, the system performance gain due to multiuser diversity is unable to compensate the total energy cost of the receivers since $K P_{C_R}$ increases linearly w.r.t. the number of receivers. Hence, the energy efficiency of the system decreases with the number of receivers. As a matter of fact, the energy efficiency gain due to the additional receivers depends on the trade-off between multiuser diversity gain, the amount of harvested energy, and the associated cost in having multiple receivers in the system. In the extreme case, when $P_{C_R} \to 0$, the energy efficiency will monotonically increase w.r.t. the number of receivers, provided that the optimization problems in (8) and (46) are feasible.

VI. CONCLUSIONS

In this paper, the resource allocation algorithm design for simultaneous wireless information and power transfer in OFDMA systems was studied. We focused on power splitting receivers which are able to split the received signals into two power streams for concurrent information decoding and energy harvesting. The algorithm design was formulated as a non-convex optimization problem which took into account a minimum system data rate requirement, minimum individual data rate requirements of the receivers, a minimum required power transfer, and the total system power dissipation. We first focused on receivers with continuous sets of power splitting ratios and proposed a resource allocation algorithm. The derived solution served as a building block for the design of a suboptimal resource allocation algorithm for receivers with discrete sets of power splitting ratios. Simulation results showed the excellent performance of the two proposed sub-optimal algorithms and also unveiled the trade-off between energy efficiency, system capacity, and wireless power transfer. In particular, wireless power transfer enhances the system energy efficiency by harvesting energy in the radio frequency, especially in the interference limited regime.

APPENDIX

VII. PROOF OF QUASI-CONCAVITY OF THE OBJECTIVE FUNCTION WITH RESPECT TO THE POWER ALLOCATION VARIABLES

For facilitating the following presentation, we first provide a definition for quasi-concave functions. Consider a function $g(\cdot)$ with input vector $\mathbf{x}$. $g(\mathbf{x})$ is a strictly quasi-concave function if and only if its super-level set [26]

$$L_\nu = \{\mathbf{x} \in \mathbf{R}^n | g(\mathbf{x}) \geq \nu\}, \ \nu \in \mathbf{R}, \tag{62}$$

is concave, where $\mathbf{R}$ denotes the set of real numbers. Suppose $g(\mathcal{P}, \mathcal{S}, \boldsymbol{\rho}) = \frac{U(\mathcal{P}, \mathcal{S}, \boldsymbol{\rho})}{U_{TP}(\mathcal{P}, \mathcal{S}, \boldsymbol{\rho})}$. Now, we focus on the following set:

$$\frac{U(\mathcal{P}, \mathcal{S}, \boldsymbol{\rho})}{U_{TP}(\mathcal{P}, \mathcal{S}, \boldsymbol{\rho})} \geq \nu. \tag{63}$$

When $\nu < 0$, the set is empty since $U(\mathcal{P}, \mathcal{S}, \boldsymbol{\rho}) > 0$ and $U_{TP}(\mathcal{P}, \mathcal{S}, \boldsymbol{\rho}) > 0$. As a result, L_α is an affine(/concave) set [26] for $\nu < 0$. Then, for $\nu > 0$, we can rewrite set L_ν as

$$\frac{U(\mathcal{P}, \mathcal{S}, \boldsymbol{\rho})}{U_{TP}(\mathcal{P}, \mathcal{S}, \boldsymbol{\rho})} \geq \nu$$
$$\iff \quad U(\mathcal{P}, \mathcal{S}, \boldsymbol{\rho}) - \nu U_{TP}(\mathcal{P}, \mathcal{S}, \boldsymbol{\rho}) \geq 0. \tag{64}$$

Since $U(\mathcal{P}, \mathcal{S}, \boldsymbol{\rho}) > 0$ and $U_{TP}(\mathcal{P}, \mathcal{S}, \boldsymbol{\rho}) > 0$ are concave and affine functions with respect to the power allocation variables $\mathcal{P}$, respectively, (64) is a concave function and L_ν represents a concave set for $\nu > 0$. Therefore, the objective function is a strictly quasi-concave function with respect to the power allocation variables. In other words, the objective function is either 1) first monotonically non-decreasing and then monotonically non-increasing or 2) monotonically non-decreasing with respect to the power allocation variables.

In the following, we show that the objective function is first monotonically non-decreasing and then monotonically non-increasing with respect to the power allocation variables. For facilitating the following analysis, we assume that subcarrier i is allocated to receiver k, i.e., $s^*_{i,k} = 1$, while $\rho^{E*}_{i,k}$ and $\rho^{I*}_{i,k}$

are given. Then, we take a partial derivative of the objective function with respect to $P_{i,k}$ which yields

$$\frac{\partial g(\mathcal{P},\mathcal{S},\boldsymbol{\rho})}{\partial P_{i,k}} = \frac{A_{i,k}}{B_{i,k}} \tag{65}$$

where $A_{i,k} = \Gamma_{i,k}\Big(\Omega_{i,k}P_{i,k} + P_{C_T} + KP_{C_R} - \sum_{k=1}^{K} Q_{I,k}\Big)$
$$\qquad - \Omega_{i,k}(1+P_{i,k}\Gamma_{i,k})\ln(1+P_{i,k}\Gamma_{i,k}),$$

$$B_{i,k} = \ln(2)(P_{i,k}\Gamma_{i,k}+1)$$
$$\qquad \times \Big(\Omega_{i,k}P_{i,k} + P_{C_T} + KP_{C_R} - \sum_{k=1}^{K} Q_{I,k}\Big)^2, \text{ and}$$

$$\Omega_{i,k} = \varepsilon - \sum_{k=1}^{K} l_k g_k |H_{i,k}|^2 \rho_{i,k}^{E*}. \tag{66}$$

We note that $\Omega_{i,k} > 0$ holds since $P_{i,k} \geq \varepsilon P_{i,k} > P_{i,k}\sum_{k=1}^{K} l_k g_k |H_{i,k}|^2$ where the strict inequality is due to the second law of thermodynamics from physics. Then, we have

$$\frac{\partial g(\mathcal{P},\mathcal{S},\boldsymbol{\rho})}{\partial P_{i,k}}\Big|_{P_{i,k}\to 0} = -\frac{W\Gamma_{i,k}}{\sum_{k=1}^{K} Q_{I_k} - P_{C_T} - KP_{C_R}} > 0 \tag{67}$$

due to $P_{C_T} + KP_{C_R} > \sum_{k=1}^{K} Q_{I_k}$. In other words, the objective function is increasing when $P_{i,k}$ increases from zero. On the other hand, when $P_{i,k}$ is sufficiently large, e.g., $P_{i,k} \to \infty$, the first partial derivative of the objective function with respect to $P_{i,k}$ is given by

$$\frac{\partial g(\mathcal{P},\mathcal{S},\boldsymbol{\rho})}{\partial P_{i,k}}\Big|_{P_{i,k}\to\infty} = \lim_{P_{i,k}\to\infty} \frac{A_{i,k}}{B_{i,k}}$$
$$\overset{(a)}{=} \lim_{P_{i,k}\to\infty} \frac{-\Omega_{i,k}\Gamma_{i,k}\log_2(1+P_{i,k}\Gamma_{i,k})}{\big(\Gamma_{i,k}(3\Omega_{i,k}P_{i,k}+P_{C_T}+KP_{C_R}-\sum_{k=1}^{K} Q_{I_k})+2\Omega_{i,k}\big)}$$
$$\qquad \times \frac{1}{(\Omega_{i,k}P_{i,k}+P_{C_T}+KP_{C_R}-\sum_{k=1}^{K} Q_{I_k})}$$
$$\leq 0, \tag{68}$$

where (a) is due to the use of L'Hospital's rule. Thus, the objective function is monotonic non-increasing for large increasing $P_{i,k}$. By combining (67) and (68), we conclude that the objective function is a quasi-concave function with respect to the power allocation variables. Specifically, it is first monotonically non-decreasing and then monotonically non-increasing with respect to $P_{i,k}$.

A. Proof of Concavity of the Transformed Problem with Objective Function Approximation

The concavity of the optimization problem with approximated objective function can be proved by the following few steps. First, we consider the concavity of function $\widehat{U}(\mathcal{P},\mathcal{S},\boldsymbol{\rho})$ on a per subcarrier basis w.r.t. the optimization variables $\tilde{P}_{i,k}$, $\tilde{\rho}_{i,k}^I$, and $\rho_{i,k}^E$. For notational simplicity, we define a vector $\mathbf{x}_{i,k} = [\tilde{P}_{i,k} \ \tilde{\rho}_{i,k}^I \ \rho_{i,k}^E]$ and a function $f_{i,k}(\mathbf{x}_{i,k}) = W\alpha_k \log_2\Big(\frac{\tilde{P}_{i,k}\tilde{\rho}_{i,k}^I l_k g_k |H_{i,k}|^2}{\tilde{\rho}_{i,k}^I(\sigma_{z^a}^2 + \sigma_{I_{i,k}}^2) + \sigma_{z^s}^2}\Big)$ which takes vector $\mathbf{x}_{i,k}$ as input. Then, we denote by $\mathbf{H}(f_{i,k}(\mathbf{x}_{i,k}))$, and τ_1, τ_2, and τ_3 the Hessian matrix of function $f_{i,k}(\mathbf{x}_{i,k})$ and the eigenvalues

of $\mathbf{H}(f_{i,k}(\mathbf{x}_{i,k}))$, respectively. The Hessian matrix of function $f_{i,k}(\mathbf{x}_{i,k})$ is given by

$$\mathbf{H}(f_{i,k}(\mathbf{x}_{i,k}))$$
$$= \begin{bmatrix} \frac{-1}{(\tilde{P}_{i,k})^2 \ln(2)} & 0 & 0 \\ 0 & \frac{-\sigma_{z^a}^2\big(\sigma_{z^a}^2 + 2\tilde{\rho}_{i,k}^I \sigma_{I_{i,k}}^2\big)}{(\tilde{\rho}_{i,k}^I)^2 \ln(2)\big(\sigma_{z^a}^2 + \tilde{\rho}_{i,k}^I \sigma_{I_{i,k}}^2\big)^2} & 0 \\ 0 & 0 & 0 \end{bmatrix} \tag{69}$$

and the corresponding eigenvalues are $\tau_1 = \frac{-1}{(\tilde{P}_{i,k})^2 \ln(2)}$, $\tau_2 = \frac{-\sigma_{z^a}^2\big(\sigma_{z^a}^2 + 2\tilde{\rho}_{i,k}^I \sigma_{I_{i,k}}^2\big)}{(\tilde{\rho}_{i,k}^I)^2 \ln(2)\big(\sigma_{z^a}^2 + \tilde{\rho}_{i,k}^I \sigma_{I_{i,k}}^2\big)^2}$, and $\tau_3 = 0$. Since $\tau_a \leq 0, a \in \{1,2,3\}$, $\mathbf{H}(f_{i,k}(\mathbf{x}_{i,k}))$ is a negative semi-definite matrix. In other words, function $f_{i,k}(\mathbf{x}_{i,k})$ is jointly concave w.r.t. $\tilde{P}_{i,k}$, $\tilde{\rho}_{i,k}^I$, and $\rho_{i,k}^E$. Then, we can perform the perspective transformation on $f_{i,k}(\mathbf{x}_{i,k})$ which is given by $u_{i,k}(\mathbf{x}_{i,k}) = s_{i,k}f_{i,k}(\mathbf{x}_{i,k}/s_{i,k})$. We note that the perspective transformation preserves the concavity of the function [26] and $u_{i,k}(\mathbf{x}_{i,k})$ is jointly concave w.r.t. $\tilde{P}_{i,k}$, $\tilde{\rho}_{i,k}^I$, $\rho_{i,k}^E$, and $s_{i,k}$. Subsequently, $\widehat{U}(\mathcal{P},\mathcal{S},\boldsymbol{\rho}) = \sum_{i=1}^{n_F}\sum_{k=1}^{K} W\alpha_k u_{i,k}(\mathbf{x}_{i,k})$ can be constructed as a non-negative weighted sum of $u_{i,k}(\mathbf{x}_{i,k})$ which guarantees the concavity of the resulting function. Besides, $\widehat{U}_{TP}(\mathcal{P},\mathcal{S},\boldsymbol{\rho})$ is an affine function of the optimization variables. Thus, $\widehat{U}(\mathcal{P},\mathcal{S},\boldsymbol{\rho}) - q\widehat{U}_{TP}(\mathcal{P},\mathcal{S},\boldsymbol{\rho})$ is jointly concave w.r.t. the optimization variables. On the other hand, constraints C1–C11 (with relaxed constraint C7), C14, and C15 span a convex feasible set. As a result, the transformed problem with the approximated objective function is a concave maximization problem.

REFERENCES

[1] D. W. K. Ng, E. Lo, and R. Schober, "Energy-efficient resource allocation in multiuser OFDM systems with wireless information and power transfer," in *Proc. 2013 IEEE Wireless Commun. and Networking Conf.*

[2] ——, "Energy-efficient power allocation in OFDM systems with wireless information and power transfer," in *Proc. 2013 IEEE Intern. Commun. Conf.*

[3] K. Pentikousis, "In search of energy-efficient mobile networking," *IEEE Commun. Mag.*, vol. 48, pp. 95–103, Jan. 2010.

[4] T. Chen, Y. Yang, H. Zhang, H. Kim, and K. Horneman, "Network energy saving technologies for green wireless access networks," *IEEE Wireless Commun.*, vol. 18, pp. 30–38, Oct. 2011.

[5] O. Arnold, F. Richter, G. Fettweis, and O. Blume, "Power consumption modeling of different base Ssation types in heterogeneous cellular networks," in *Proc. 2010 Future Network and Mobile Summit*, pp. 1–8.

[6] J. Yang and S. Ulukus, "Optimal packet scheduling in an energy harvesting communication system," *IEEE Trans. Commun.*, vol. 60, pp. 220–230, Jan. 2012.

[7] D. W. K. Ng, E. Lo, and R. Schober, "Energy-efficient resource allocation in OFDMA systems with large numbers of base station antennas," *IEEE Trans. Wireless Commun.*, vol. 11, pp. 3292–3304, Sep. 2012.

[8] F. Zhang, S. Hackworth, X. Liu, H. Chen, R. Sclabassi, and M. Sun, "Wireless energy transfer platform for medical sensors and implantable devices," in *Proc. 2009 Intern. Conf. of the IEEE Eng. in Med. and Biol. Soc.*, pp. 1045–1048.

[9] V. Chawla and D. S. Ha, "An overview of passive RFID," *IEEE Commun. Mag.*, vol. 45, pp. 11–17, Sep. 2007.

[10] L. Varshney, "Transporting information and energy simultaneously," in *Proc. 2008 IEEE Intern. Sympos. on Inf. Theory*, pp. 1612–1616.

[11] P. Grover and A. Sahai, "Shannon meets Tesla: wireless information and power transfer," in *Proc. 2010 IEEE Intern. Sympos. on Inf. Theory*, pp. 2363–2367.

[12] R. Zhang and C. K. Ho, "MIMO broadcasting for simultaneous wireless information and power transfer," in *Proc. 2011 IEEE Global Telecommun. Conf.*, pp. 1–5.

[13] L. Liu, R. Zhang, and K.-C. Chua, "Wireless information transfer with opportunistic energy harvesting," *IEEE Trans. Wireless Commun.*, vol. 3, pp. 345–362, Jan. 2013.

[14] X. Zhou, R. Zhang, and C. K. Ho, "Wireless information and power transfer: architecture design and rate-energy tradeoff," *IEEE Trans. Commun.*, vol. PP, 2013.

[15] C. Isheden, Z. Chong, E. Jorswieck, and G. Fettweis, "Framework for link-level energy efficiency optimization with informed transmitter," *IEEE Trans. Wireless Commun.*, vol. 11, pp. 2946–2957, Aug. 2012.

[16] G. Miao, N. Himayat, and G. Li, "Energy-efficient link adaptation in frequency-selective channels," *IEEE Trans. Commun.*, vol. 58, pp. 545–554, Feb. 2010.

[17] F. Philipp, P. Zhao, F. Samman, M. Glesner, K. Dassanayake, S. Maheswararajah, and S. Halgamuge, "Adaptive wireless sensor networks powered by hybrid energy harvesting for environmental monitoring," in *Proc. 2012 IEEE Intern. Conf. on Inf. and Autom. for Sustainability*, pp. 285–289.

[18] A. Iyer, C. Rosenberg, and A. Karnik, "What is the right model for wireless channel interference?" *IEEE Trans. Wireless Commun.*, vol. 8, pp. 2662–2671, May 2009.

[19] Y. Ma, A. Leith, M.-S. Alouini, and X. Shen, "Weighted-SNR-based fair scheduling for uplink OFDMA," in *Proc. 2009 IEEE Global Telecommun. Conf.*, pp. 1–6.

[20] G. Song and Y. Li, "Cross-layer optimization for OFDM wireless networks—part II: algorithm development," *IEEE Trans. Wireless Commun.*, vol. 4, pp. 625–634, Mar. 2005.

[21] D. W. K. Ng and R. Schober, "Resource allocation and scheduling in multi-cell OFDMA systems with decode-and-forward relaying," *IEEE Trans. Wireless Commun.*, vol. 10, pp. 2246–2258, Jul. 2011.

[22] W. Dinkelbach, "On nonlinear fractional programming," *Management Science*, vol. 13, pp. 492–498, Mar. 1967. Available: http://www.jstor.org/stable/2627691

[23] T. Ibarako, "Parametric approaches to fractional programs," *Mathematical Programming*, vol. 26, pp. 288–300, Jan. 1983.

[24] C. Y. Wong, R. S. Cheng, K. B. Letaief, and R. D. Murch, "Multiuser OFDM with adaptive subcarrier, bit, and power allocation," *IEEE J. Sel. Areas Commun.*, vol. 17, pp. 1747–1758, Oct. 1999.

[25] W. Yu and R. Lui, "Dual methods for nonconvex spectrum optimization of multicarrier systems," vol. 54, pp. 1310–1321, July 2006.

[26] S. Boyd and L. Vandenberghe, *Convex Optimization*. Cambridge University Press, 2004.

[27] K. Seong, M. Mohseni, and J. Cioffi, "Optimal resource allocation for OFDMA downlink systems," in *Proc. 2006 IEEE Intern. Sympos. on Inf. Theory*, pp. 1394–1398.

[28] S. Boyd, L. Xiao, and A. Mutapcic, "Subgradient methods," *Notes for EE392o Stanford University Autumn*, 2003-2004.

[29] IEEE P802.11 Wireless LANs, "TGn Channel Models," IEEE 802.11-03/940r4, Tech. Rep., May 2004.

[30] F. Wang, A. Ojo, D. Kimball, P. Asbeck, and L. Larson, "Envelope tracking power amplifier with pre-distortion linearization for WLAN 802.11g," in *2004 IEEE MTT-S Intern. Microw. Symposium Digest*, pp. 1543–1546.

[31] H.-S. Chen and W. Gao, "MAC and PHY proposal for 802.11af," Tech. Rep., Feb. Available: https://mentor.ieee.org/802.11/dcn/10/11-10-0258-00-00af-mac-and-phy-proposal-for-802-11af.pdf.

[32] D. P. Bertsekas, *Nonlinear Programming*, 2nd ed. Athena Scientific, 1999.

Derrick Wing Kwan Ng (S'06-M'12) received the bachelor degree with first class honors and the Master of Philosophy (M.Phil.) degree in electronic engineering from the Hong Kong University of Science and Technology (HKUST) in 2006 and 2008, respectively. He received his Ph.D. degree from the University of British Columbia (UBC) in 2012. In the summer of 2011 and spring of 2012, he was a visiting scholar at the Centre Tecnològic de Telecomunicacions de Catalunya - Hong Kong (CTTC-HK). He is now working as a postdoctoral fellow in the Institute for Digital Communications, Friedrich-Alexander-University Erlangen-Nürnberg (FAU), Germany. His research interests include cross-layer optimization for wireless communication systems, resource allocation in OFDMA wireless systems, and communication theory.

Dr. Ng received the Best Paper Awards at the IEEE Wireless Communications and Networking Conference (WCNC) 2012, the IEEE Global Telecommunication Conference (Globecom) 2011, and the IEEE Third International Conference on Communications and Networking in China 2008. He was awarded the IEEE Student Travel Grants for attending the IEEE WCNC 2010, the IEEE International Conference on Communications (ICC) 2011, and the IEEE Globecom 2011. He was also the recipient of the 2009 Four Year Doctoral Fellowship from the UBC, Sumida & Ichiro Yawata Foundation Scholarship in 2008, and R&D Excellence Scholarship from the Center for Wireless Information Technology in HKUST in 2006. He has served as an editorial assistant to the Editor-in-Chief of the IEEE TRANSACTIONS ON COMMUNICATIONS since Jan. 2012. He is currently an Editor of the IEEE COMMUNICATIONS LETTERS. He has been a TPC member of various conferences, including the Globecom, WCNC, ICC, and PIMRC, etc. He was honoured as an Exemplary Reviewer of the IEEE Wireless Communications Letters in 2013.

Ernest S. Lo (S'02-M'08) is the Founding Director and Chief Representative of the Centre Tecnolgic de Tecnològic de Catalunya - Hong Kong (CTTC-HK). He was a Croucher Postdoc Fellow at Stanford University, and received his Ph.D., M.Phil., and B.Eng. (1st Hons.) from the Hong Kong University of Science and Technology. He has a broad spectrum of research interests, including channel coding, resource allocation, and wireless system and architectural design, all with a goal of finding new resources and inventing new technologies for realizing a flexible, spectrally-efficient, and energy-efficient wireless multiuser network. He contributed to the standardization of the IEEE 802.22 cognitive radio WRAN system and holds a few pending and granted US and China patents. Some of them were transferred to other companies.

Dr. Lo has received three Best Paper Awards, one at the IEEE International Conference on Communications (ICC) 2007, Glasgow, and another two at the IEEE Global Communications Conference (GLOBECOM), 2011, Houston, and the IEEE Wireless Communications and Networking Conference (WCNC) 2012, Paris, respectively. He served as an Editorial Assistant of the IEEE TRANSACTIONS ON WIRELESS COMMUNICATIONS when it was founded and has been a TPC member of various conferences, including the IEEE ICC'10,11,12, IEEE GLOBECOM'10,11,12, and IEEE ICCC'12, etc. He was honoured as an Exemplary Reviewer of the IEEE Communications Letters.

Robert Schober (M'01, SM'08, F'10) was born in Neuendettelsau, Germany, in 1971. He received the Diplom (Univ.) and the Ph.D. degrees in electrical engineering from the University of Erlangen-Nuermberg in 1997 and 2000, respectively. From May 2001 to April 2002 he was a Postdoctoral Fellow at the University of Toronto, Canada, sponsored by the German Academic Exchange Service (DAAD). Since May 2002 he has been with the University of British Columbia (UBC), Vancouver, Canada, where he is now a Full Professor. Since January 2012 he is an Alexander von Humboldt Professor and the Chair for Digital Communication at the Friedrich Alexander University (FAU), Erlangen, Germany. His research interests fall into the broad areas of Communication Theory, Wireless Communications, and Statistical Signal Processing.

Dr. Schober received the 2002 Heinz MaierLeibnitz Award of the German Science Foundation (DFG), the 2004 Innovations Award of the Vodafone Foundation for Research in Mobile Communications, the 2006 UBC Killam Research Prize, the 2007 Wilhelm Friedrich Bessel Research Award of the Alexander von Humboldt Foundation, the 2008 Charles McDowell Award for Excellence in Research from UBC, a 2011 Alexander von Humboldt Professorship, and a 2012 NSERC E.W.R. Steacie Fellowship. In addition, he received best paper awards from the German Information Technology Society (ITG), the European Association for Signal, Speech and Image Processing (EURASIP), IEEE WCNC 2012, IEEE Globecom 2011, IEEE ICUWB 2006, the International Zurich Seminar on Broadband Communications, and European Wireless 2000. Dr. Schober is a Fellow of the Canadian Academy of Engineering and a Fellow of the Engineering Institute of Canada. He is currently the Editor-in-Chief of the IEEE TRANSACTIONS ON COMMUNICATIONS.